Lepton Flavour Violation in minimal grand-unified type II seesaw models

Lorenzo Calibbi $^{\dagger 1}$ and Xiyuan Gao $^{\star 2}$

- [†] School of Physics, Nankai University, Tianjin 300071, China
- * Arnold-Sommerfeld-Center, Ludwig-Maximilians-Universität, München 80333, Germany

Abstract

We revisit minimal non-supersymmetric models of SU(5) Grand Unification with the type II seesaw mechanism as the origin of neutrino masses. Imposing the requirement of gauge coupling unification and the proton lifetime bounds, we perform a Bayesian fit and obtain robust quantitative information on the mass scales of the beyond the Standard Model particles. We then study lepton-flavour-violating (LFV) processes induced by the type II scalar triplet and its SU(5) partners, showing that the interplay of upcoming searches for different LFV observables can provide additional information on the masses of the new particles, as well as non-trivial constraints on neutrino parameters.

¹calibbi@nankai.edu.cn

²Xiyuan.Gao@campus.lmu.de

Contents

1	Introduction	2
2	Minimal models of Grand Unification with type II seesaw	3
3	Fit of the mass spectrum of minimal models	7
4	Type II seesaw fields and Lepton Flavour Violation	15
5	Summary and conclusions	24
\mathbf{A}	Scalar potential and scalar mass spectrum	25
В	More details on proton decay	2 6
\mathbf{C}	RGEs of triplet and leptoquark Yukawa couplings	2 8
D	Dependence of the LFV rates on neutrino parameters	28

1 Introduction

Grand Unification is a powerful guiding principle towards unveiling new physics beyond the Standard Model (SM). The coupling constants of the three SM interactions exhibit the tendency to unify to a common value at a very high energy scale $M_{\rm GUT}$. This has been long regarded as a hint for a Grand Unified Theory (GUT) where the SM gauge group $SU(3)_c \times SU(2)_L \times U(1)_Y$ is embedded in a simple gauge group, such as SU(5) or SO(10) [1, 2]. This paradigm is very appealing for a number of theoretical and phenomenological reasons—for a recent review, see [3]. In particular, GUTs give a rationale behind the otherwise unexplained quantum numbers of the SM fermions, thus accounting for the quantisation of the electric charge and the exact cancellation of gauge anomalies within each single generation of fermions. Furthermore, since quarks and leptons are embedded in common irreducible representations of the GUT group, interactions mediated by GUT gauge bosons unavoidably violate baryon and lepton number, making GUT models in principle testable by searches for proton decay.

For what concerns the following discussion, even more important is the observation that the contributions to the running of the gauge couplings due to the SM field content alone can not achieve a successful unification. Hence GUTs provide a strong motivation for the presence of new fields at intermediate or low-energy scales that can prompt gauge coupling unification. Other open problems of the SM, in particular the origin of neutrino masses, nicely lead to the same conclusion. It is therefore very tempting to look for the fields able to account for gauge coupling unification among those responsible for neutrino masses. However, that does not seem straightforward within the context of the simplest extensions of the SM addressing neutrino masses — Dirac neutrinos or Majorana neutrinos from type I seesaw — as they only involve singlet representations of the SM gauge group (the right-handed neutrinos) that (i) do not affect the running of the gauge couplings themselves, and (ii) are naturally embedded in GUT representations that do not comprise extra fields which could facilitate unification (as they are singlets within SU(5) too, while they nicely fit the 16 spinorial representation of SO(10)together with the other SM fermions). Thus, the programme of achieving a minimal connection between neutrino mass models and unification should rather focus on the other two types of seesaw mechanism or on radiative neutrino mass models.

¹For a comprehensive discussion of the low-energy phenomenology of the former, see [4], while for a review on the latter we refer to [5].

In this paper, we focus on what is perhaps the simplest possibility, type II seesaw [6–9], that is, we are going to introduce a single scalar $SU(2)_L$ triplet and its SU(5) partners contained in the **15** representation. Requiring a successful gauge coupling unification and enforcing the proton decay bound set non-trivial constraints on the masses of these new particles, leading to interesting and potentially testable phenomenological consequences. This has been extensively studied in the literature [10–16], with a particular focus on the possibility that some states are light enough to be within the reach of high-energy colliders, such as the Large Hadron Collider (LHC).²

In the following, we revisit several variations of the SU(5) embedding of type II seesaw (distinguished by the way employed to fix the "wrong" fermion mass relations predicted by the minimal Georgi-Glashow SU(5) model [1], see Section 2) and extend the existing literature in multiple directions. We first perform a Bayesian fit to the gauge coupling unification requirement and the proton lifetime constraint, in order to obtain reliable quantitative information about the viable spectrum of the theory (Section 3) and compare it with direct searches for new physics at the LHC. In Section 4, we move to what is the main focus of the paper: the study of charged lepton-flavour-violating (LFV) decays that are induced by the fields contained in the 15, which are unavoidable since the couplings of these fields to the SM fermions need to account for the observed neutrino masses and mixing and must thus be flavour-changing (and are to large extent known). Searches for LFV decays are among the most sensitive probes of new physics coupling to SM leptons. In particular, the ongoing experimental programme is capable to reach scales exceeding $10^7 - 10^8$ GeV [24]. We are going to study the potential of future experiments of testing type II seesaw GUT models and highlight how the interplay of different LFV observables can provide information on the masses of the new particles, as well as complementary constraints on the neutrino parameters that have not been measured yet.

2 Minimal models of Grand Unification with type II seesaw

We start from the minimal non-supersymmetric SU(5) Georgi-Glashow model [1], with the SM fermions organised within the first two lowest-dimension SU(5) representations ($\overline{\bf 5}$ and ${\bf 10}$):

$$\psi_{\bar{5}} = (D_R)^c (\bar{3}, 1, 1/3) \oplus L_L (1, 2, -1/2),$$
 (1)

$$\psi_{10} = Q_L(\mathbf{3}, \mathbf{1}, 1/6) \oplus (U_R)^c(\mathbf{\bar{3}}, \mathbf{1}, -2/3) \oplus (E_R)^c(\mathbf{1}, \mathbf{1}, 1),$$
(2)

where the $SU(3)_c \times SU(2)_L \times U(1)_Y$ quantum numbers are shown in parenthesis.

The scalar sector consists of the real field ϕ_{24} in a 24-dimensional representation and the 5-dimensional ϕ_{5} (the latter one containing the SM Higgs doublet), whose vevs cause the two-step spontaneous breaking $SU(5) \xrightarrow{v_{24}} SU(3)_c \times SU(2)_L \times U(1)_Y \xrightarrow{v_5} SU(3)_c \times U(1)_{em}$. The SM gauge bosons are also contained in an adjoint representation of SU(5), together with new ones (the vector leptoquarks (3, 2, 5/6) and $(\overline{3}, 2, -5/6)$, typically denoted as X^{μ} , Y^{μ}) that convert quarks into leptons, thus inducing proton decay. The mass of these latter fields is proportional to the GUT-breaking vev v_{24} and, in the following, we are going to identify it with the unification scale M_{GUT} where the three gauge couplings meet (and employ such an assumption to assess the impact of the extra gauge bosons on the proton lifetime, see Section 3). In other words, we are assuming that X^{μ} and Y^{μ} do not contribute to the running of the gauge couplings below the unification scale. Similarly, we are also assuming that the mass of the colour triplet in ϕ_5 is at the GUT scale or above. In fact, this field does not only give rise to additional, potentially dangerous, contributions to proton decay (that typically bound its mass to be $\gtrsim 10^{11}$ GeV) but also tends to spoil the successful unification of the gauge couplings [10].

²For analogous studies within the context of type III seesaw, see [17–22], while a general discussion on gauge coupling unification due to intermediate-scale scalar fields can be found in Ref. [23].

On the other hand, we will allow (some of) the states belonging to the SU(5)-breaking Higgs field ϕ_{24} to have masses lighter than M_{GUT} , so to trigger gauge coupling unification. Notice, however, that this can not be the case of the scalar states $(\mathbf{3}, \mathbf{2}, 5/6)$ and $(\mathbf{\bar{3}}, \mathbf{2}, -5/6)$ that are just the would-be Goldstone bosons from SU(5) breaking and provide the longitudinal components of the GUT gauge bosons X^{μ} , Y^{μ} .

Within the minimal SU(5) model, such as in the Standard Model, neutrinos are massless, which conflicts with the observation of neutrino oscillations. As anticipated in the introduction, we assume that neutrino masses arise from the seesaw mechanism of type II, which requires the introduction of a scalar triplet Δ with lepton-number-breaking interactions [6–9].³ The simplest representation of SU(5) where this field can fit in is the 15 whose SM decomposition also contains a scalar leptoquark that, as customary, we denote as \widetilde{R}_2 (see e.g. the review in Ref. [27]) and a scalar colour sextet S [10]:

$$\phi_{15} = \Delta(1, 3, 1) \oplus \widetilde{R}_2(3, 2, 1/6) \oplus S(6, 1, -2/3).$$
 (3)

The SU(5) Lagrangian of the Yukawa sector thus reads:

$$-\mathcal{L}_{\text{Yukawa}} = Y_{u} \epsilon_{ijklm} \overline{\psi_{\mathbf{10}}^{ij}} (\psi_{\mathbf{10}}^{kl})^{c} \phi_{\mathbf{5}}^{m*} + Y_{d\ell} \phi_{\mathbf{5}}^{i} \overline{\psi_{\mathbf{10}}^{ij}} (\psi_{\overline{\mathbf{5}}}^{j})^{c} + Y_{15} \overline{\psi_{\overline{\mathbf{5}}}^{i}} \phi_{\mathbf{15}}^{ij*} (\psi_{\overline{\mathbf{5}}}^{j})^{c} + \text{h.c.},$$
(4)

where i, j, k, l, m = 1 - 5 are SU(5) indices, ϵ_{ijklm} is a rank-5 totally antisymmetric tensor, Y_u , $Y_{d\ell}$, and Y_{15} are 3×3 matrices of Yukawa couplings, whose flavour indices are not explicitly shown. The Y_{15} terms give mass to neutrinos via type II seesaw in the usual way, see the discussion in Section 4.

As is well known, the second term in Eq. (4) predicts the following GUT-scale relations among lepton and down-type quark masses:

$$m_d = m_e \,, \ m_s = m_\mu \,, \ m_b = m_\tau \,, \qquad [minimal \ SU(5)]$$
 (5)

which are notoriously at odds with the experimental measurements, even taking into account the renormalisation group running down to the electroweak scale [28, 29]. Several ways to correct these relations have been proposed in the literature. In the following, we will review three popular choices and employ them to identify the possible minimal sets of fields that can provide phenomenologically viable fermion masses (including neutrino ones).

Model 1: non-renormalisable operators. The simplest way to fix the quark-lepton mass relations shown in Eq. (5) is to add the following non-renormalisable operators [10, 13, 30]:

$$-\mathcal{L}_{\text{Yukawa}} \supset \frac{Y'_{u}}{\Lambda} \epsilon_{ijklm} \overline{\psi_{\mathbf{10}}^{ij}} (\psi_{\mathbf{10}}^{kl})^{c} \phi_{\mathbf{24}}^{mn} \phi_{\mathbf{5}}^{n*} + \frac{Y''_{u}}{\Lambda} \epsilon_{ijklm} \overline{\psi_{\mathbf{10}}^{ij}} (\psi_{\mathbf{10}}^{kn})^{c} \phi_{\mathbf{24}}^{mn} \phi_{\mathbf{5}}^{l*} \\ + \frac{Y'_{d\ell}}{\Lambda} \phi_{\mathbf{5}}^{i} \overline{\psi_{\mathbf{10}}^{ij}} \phi_{\mathbf{24}}^{jk} (\psi_{\mathbf{\overline{5}}}^{k})^{c} + \frac{Y''_{d\ell}}{\Lambda} \phi_{\mathbf{5}}^{i} \phi_{\mathbf{24}}^{ij} \overline{\psi_{\mathbf{10}}^{jk}} (\psi_{\mathbf{\overline{5}}}^{k})^{c} + \text{h.c.},$$
(6)

where $\Lambda \gg M_{\text{GUT}}$, implying some new degrees of freedom beyond minimal SU(5) (e.g. at the Planck scale). From Eqs. (4, 6), one obtains the following Yukawa terms after SU(5) breaking:

$$-\mathcal{L}_{\text{Mass}} \supset 4\overline{Q_L}(Y_u + Y_u^T)\widetilde{H}U_R + \overline{Q_L}Y_{d\ell}HD_R + \overline{L_L}Y_{d\ell}^THE_R$$

$$-\frac{6v_{24}}{\Lambda}\overline{Q_L}(Y_u' + Y_u'^T)\widetilde{H}U_R + \frac{v_{24}}{\Lambda}\overline{Q_L}Y_{d\ell}'HD_R - \frac{3v_{24}}{2\Lambda}\overline{L_L}Y_{d\ell}'^THE_R$$

$$-\frac{v_{24}}{\Lambda}\overline{Q_L}(Y_u'' - Y_u''^T)\widetilde{H}U_R - \frac{3v_{24}}{2\Lambda}\overline{Q_L}Y_{d\ell}''HD_R - \frac{3v_{24}}{2\Lambda}\overline{L_L}Y_{d\ell}''^THE_R + \text{h.c.},$$
(7)

³Interestingly, type II seesaw can also successfully address leptogenesis and inflation [25, 26].

which give for the fermion mass matrices

$$M_{u} = 2\sqrt{2}v_{5}\left(Y_{u} + Y_{u}^{T} - \frac{3v_{24}}{2\Lambda}Y_{u}^{\prime} - \frac{3v_{24}}{2\Lambda}Y_{u}^{\prime T} - \frac{v_{24}}{4\Lambda}Y_{u}^{\prime\prime} + \frac{v_{24}}{4\Lambda}Y_{u}^{\prime\prime T}\right),$$

$$M_{d} = \frac{v_{5}}{\sqrt{2}}\left(Y_{d\ell} + \frac{v_{24}}{\Lambda}Y_{d\ell}^{\prime} - \frac{3v_{24}}{2\Lambda}Y_{d\ell}^{\prime\prime}\right), \quad M_{\ell} = \frac{v_{5}}{\sqrt{2}}\left(Y_{d\ell}^{T} - \frac{3v_{24}}{2\Lambda}Y_{d\ell}^{\prime T} - \frac{3v_{24}}{2\Lambda}Y_{d\ell}^{\prime\prime T}\right).$$
(8)

The presence of the additional contributions $\propto Y'_{d\ell}$, $Y''_{d\ell}$ clearly breaks the minimal relations of Eq. (5), allowing to fit the observed fermion masses by suitably adjusting the entries of the matrices $Y_{d\ell}$, $Y'_{d\ell}$ and $Y''_{d\ell}$.

In summary, in the case of Model 1, the only states that, if lighter than M_{GUT} , can possibly trigger gauge-coupling unification are those contained in ϕ_{15} and ϕ_{24} [10, 11], which we display in the first block of Table 1. The conditions required in order to have some of these fields much lighter than the GUT scale or, in other words, large mass splittings in the scalar sector (which will necessarily involve fine tunings), are discussed in Appendix A.

Model 2: scalar 45. If one prefers to work within a renormalisable theory, the simplest choice is to add a 45-dimensional scalar representation [14]:

$$\phi_{45} = \varphi_8(8, \mathbf{2}, 1/2) \oplus \varphi_{\overline{6}}(\overline{\mathbf{6}}, \mathbf{1}, -1/3) \oplus \varphi_3^T(\mathbf{3}, \mathbf{3}, -1/3) \oplus \varphi_3^D(\overline{\mathbf{3}}, \mathbf{2}, -7/6) \oplus \varphi_3^S(\mathbf{3}, \mathbf{1}, -1/3) \oplus \varphi_{\overline{3}}^S(\overline{\mathbf{3}}, \mathbf{1}, 4/3) \oplus H_2(\mathbf{1}, \mathbf{2}, 1/2).$$
(9)

The additional terms in the Lagrangian of the Yukawa sector read:

$$-\mathcal{L}_{\text{Yukawa}} \supset Y_{u} \epsilon_{ijklm} \overline{\psi_{\mathbf{10}}^{ij}} (\psi_{\mathbf{10}}^{kl})^{c} \phi_{\mathbf{5}}^{m*} + Y_{d\ell} \phi_{\mathbf{5}}^{i} \overline{\psi_{\mathbf{10}}^{ij}} (\psi_{\mathbf{5}}^{j})^{c} + Y_{u}' \epsilon_{ijklm} \overline{\psi_{\mathbf{10}}^{ij}} (\psi_{\mathbf{10}}^{nk})^{c} \phi_{\mathbf{45}}^{lmn*} + Y_{d\ell}' \phi_{\mathbf{45}}^{ijk} \overline{\psi_{\mathbf{10}}^{ij}} (\psi_{\mathbf{5}}^{k})^{c} + \text{h.c.}.$$
(10)

Notice that ϕ_{45} is a rank 3 tensor, satisfying antisymmetric and traceless conditions: $\phi_{45}^{ijk} = -\phi_{45}^{jik}$, $\sum_{j=1}^{5} \phi_{45}^{ijj} = 0$. So we can choose for its vev:

$$\langle \phi_{45}^{5ij} \rangle = -\langle \phi_{45}^{i5j} \rangle = \frac{1}{\sqrt{2}} v_{45} (4\delta^{i4}\delta^{j4} - \delta^{ij}), \qquad (i, j = 1 - 4),$$
 (11)

with other entries vanishing. The fermion mass terms then result:

$$-\mathcal{L}_{\text{Mass}} \supset 4\overline{Q_L}(Y_u + Y_u^T)\widetilde{H}U_R + \overline{Q_L}Y_{d\ell}HD_R + \overline{L_L}Y_{d\ell}^THE_R - 8\overline{Q_L}(Y_u' - {Y_u'}^T)\widetilde{H_2}U_R - 6\overline{Q_L}Y_{d\ell}'H_2D_R + 2\overline{L_L}Y_{d\ell}'^TH_2E_R + \text{h.c.},$$
(12)

and one can get the following fermion mass matrices:

$$M_{u} = \frac{1}{\sqrt{2}} \left[4 \left(Y_{u} + Y_{u}^{T} \right) v_{5} - 8 \left(Y_{u}^{\prime} - Y_{u}^{\prime T} \right) v_{45}^{*} \right] ,$$

$$M_{d} = \frac{1}{\sqrt{2}} \left(v_{5} Y_{d\ell} + 2 v_{45} Y_{d\ell}^{\prime} \right) , \quad M_{\ell} = \frac{1}{\sqrt{2}} \left(v_{5} Y_{d\ell}^{T} - 6 v_{45} Y_{d\ell}^{\prime T} \right) .$$

$$(13)$$

Again, it is apparent that the entries M_u, M_d, M_ℓ are all free parameters, such that the observed fermion masses and mixing can be easily fitted.⁴ It is worth noting that at low energies this is just a two Higgs-doublet model (2HDM) with v_{45} of the order of the electroweak (EW) scale, and $v_{\rm EW} = \sqrt{v_5^2 + v_{45}^2} \approx 246$ GeV.

For this model, the extra fields possibly contributing to the running of the SM gauge couplings are those in ϕ_{15} , ϕ_{24} , and ϕ_{45} , see Table 1. Details about masses and vevs of these scalar states can be found in Appendix A.

⁴For a different approach, with the same field content as Model 2 (including the **45**) but employing non-renormalisable instead of renormalisable operators to correct Eq. (5), see Ref. [16].

All models							
Field	SU(5)	$SU(3)_c$	$SU(2)_L$	$U(1)_Y$	b_3^I	b_2^I	b_1^I
ϱ_3	ϕ_{24}	1	3	0	0	1/3	0
ϱ_8	ϕ_{24}	8	1	0	1/2	0	0
Δ	ϕ_{15}	1	3	1	0	2/3	3/5
$\widetilde{R_2}$	ϕ_{15}	3	2	1/6	1/3	1/2	1/30
S	ϕ_{15}	6	1	-2/3	5/6	0	8/15
			Model 2	2			
Field	SU(5)	$SU(3)_c$	$SU(2)_L$	$U(1)_Y$	b_3^I	b_2^I	b_1^I
$arphi_8$	ϕ_{45}	8	2	1/2	2	4/3	4/5
$\varphi_{\overline{6}}$	ϕ_{45}	$\bar{6}$	1	-1/3	5/6	0	2/15
$arphi_3^T$	ϕ_{45}	3	3	-1/3	1/2	2	1/5
φ_3^D	ϕ_{45}	$ar{3}$	2	-7/6	1/3	1/2	49/30
$arphi_3^S$	ϕ_{45}	3	1	-1/3	1/6	0	1/15
$\varphi^S_{\overline{3}}$	ϕ_{45}	$\bar{3}$	1	4/3	1/6	0	16/15
H_2	ϕ_{45}	1	2	1/2	0	1/6	1/10
			Model 3	3			
Field	SU(5)	$SU(3)_c$	$SU(2)_L$	$U(1)_Y$	b_3^I	b_2^I	b_1^I
L_V	$\psi^{\underline{v}}_{\overline{f 5}}$	1	2	-1/2	0	1/3	1/5
D_V^c	$\psi^{\underline{v}}_{\overline{f 5}}$	$ar{3}$	1	1/3	1/3	0	2/15
L_V^c	$\psi^v_{f 5}$	1	2	1/2	0	1/3	1/5
D_V	$\psi^v_{f 5}$	3	1	-1/3	1/3	0	2/15
Q_V	ψ^v_{10}	3	2	1/6	2/3	1	1/15
U_V^c	ψ^v_{10}	$\bar{3}$	1	-2/3	1/3	0	8/15
E_V^c	ψ^v_{10}	1	1	1	0	0	2/5
Q_V^c	$\psi^{\underline{v}}_{\overline{f 10}}$	$\bar{3}$	2	-1/6	2/3	1	1/15
U_V	$\psi^{\underline{v}}_{\overline{10}}$	3	1	2/3	1/3	0	8/15
E_V	$\psi^{\underline{v}}_{\overline{10}}$	1	1	-1	0	0	2/5

Table 1: New fields with mass possibly below M_{GUT} , the corresponding group representations, and their contribution to the one-loop β function coefficients of the SM gauge couplings.

Model 3: vector-like fermions. The last possibility we consider is adding heavy fermions in vector-like representations of SU(5) (and thus of the SM gauge group too) [31, 32], that is, the $\mathbf{5} \oplus \mathbf{\bar{5}}$ representation:

$$\psi_{\overline{5}}^{v} = D_{V}^{c}(\overline{3}, \mathbf{1}, 1/3) \oplus L_{V}(\mathbf{1}, \mathbf{2}, -1/2),
\psi_{\overline{5}}^{v} = D_{V}(\mathbf{3}, \mathbf{1}, -1/3) \oplus L_{V}^{c}(\mathbf{1}, \mathbf{2}, 1/2),$$
(14)

and/or $\mathbf{10} \oplus \overline{\mathbf{10}}$:

$$\psi_{\mathbf{10}}^{v} = Q_{V}(\mathbf{3}, \mathbf{2}, 1/6) \oplus U_{V}^{c}(\overline{\mathbf{3}}, \mathbf{1}, -2/3) \oplus E_{V}^{c}(\mathbf{1}, \mathbf{1}, 1),
\psi_{\overline{\mathbf{10}}}^{v} = Q_{V}^{c}(\overline{\mathbf{3}}, \mathbf{2}, -1/6) \oplus U_{V}(\mathbf{3}, \mathbf{1}, 2/3) \oplus E_{V}(\mathbf{1}, \mathbf{1}, -1).$$
(15)

These vector-like pairs of Weyl fermions combine into Dirac fermions that, with slight abuse of notation, we will also denote as $\psi^v_{\overline{\bf 5}}$ and $\psi^v_{{f 10}}$.

The components of the above SU(5) fields mix with SM leptons and quarks differently, thus correcting the mass relations in Eq. (5). For example, with only one generation of vector-like fermions $\psi_{\overline{s}}^v$, the Lagrangian of the Yukawa sector becomes (in 4-component notation):

$$-\mathcal{L}_{\text{Yukawa}} \supset \left(\begin{array}{cc} \overline{\psi_{\mathbf{5}}^{\alpha}} & \overline{\psi_{\mathbf{5}}^{v}} \end{array} \right) \left(\begin{array}{cc} Y_{d\ell}^{\alpha\beta} \phi_{\mathbf{5}}^{*} & M_{5}^{\alpha} + \lambda_{5}^{\alpha} \phi_{\mathbf{24}} \\ Y_{d\ell}^{\prime\beta} \phi_{\mathbf{5}}^{*} & M_{5}^{V} + \lambda_{5}^{V} \phi_{\mathbf{24}} \end{array} \right) \left(\begin{array}{c} (\psi_{\mathbf{10}}^{\beta})^{c} \\ \psi_{\mathbf{5}}^{v} \end{array} \right) + \text{h.c.}$$

$$\rightarrow \left(\begin{array}{cc} \overline{(D_{R}^{\alpha})^{c}} & \overline{D_{V}^{c}} \end{array} \right) \left(\begin{array}{c} \frac{1}{\sqrt{2}} v_{5} Y_{d\ell}^{\alpha\beta} & M_{5}^{\alpha} + \lambda_{5}^{\alpha} v_{24} \\ \frac{1}{\sqrt{2}} v_{5} Y_{d\ell}^{\prime\beta} & M_{5}^{V} + \lambda_{5}^{V} v_{24} \end{array} \right) \left(\begin{array}{c} (D_{L}^{\beta})^{c} \\ D_{V}^{c} \end{array} \right) + \left(\begin{array}{c} \overline{E_{L}^{\alpha}} & \overline{E_{V}^{\prime}} \end{array} \right) \left(\begin{array}{c} \frac{1}{\sqrt{2}} v_{5} Y_{d\ell}^{\alpha\beta} & M_{5}^{\alpha} - \frac{3}{2} \lambda_{5}^{\alpha} v_{24} \\ \frac{1}{\sqrt{2}} v_{5} Y_{d\ell}^{\prime\beta} & M_{5}^{V} - \frac{3}{2} \lambda_{5}^{V} v_{24} \end{array} \right) \left(\begin{array}{c} E_{R}^{\beta} \\ E_{V}^{\prime} \end{array} \right),$$

$$(16)$$

where α and β are flavour indices, D_L and E_L respectively denote the down-type quarks and charged leptons in the doublets Q_L and L_L , and E'_V is the charged state in L_V .

As we can see, in addition to the standard interactions with SM fermions and Higgs fields, the vector-like fermion can also couple to chiral fermions (or itself) directly or via the SU(5) adjoint scalar field ϕ_{24} . So after spontaneous symmetry breaking, the two mass matrices for charged leptons and down-type quarks acquire six independent parameters: $(M_5^{\alpha} + \lambda_5^{\alpha} v_{24})/(M_5^V + \lambda_5^V v_{24})$ and $(M_5^{\alpha} - \frac{3}{2}\lambda_5^{\alpha} v_{24})/(M_5^V - \frac{3}{2}\lambda_5^V v_{24})$, the contribution from $\phi_5^* \overline{\psi_5^v} (\psi_{10}^{\beta})^c$ being negligible since $v_5 \ll v_{24}, M_5$. For a detailed discussion, see Ref. [33]. Therefore, one can correct the wrong quark-lepton mass relations with only one generation of vector-like fermions ψ_5^v .

The above result can be straightforwardly generalised to the ψ_{10}^v case:.

$$-\mathcal{L}_{\text{Yukawa}} \supset \left(\begin{array}{cc} \overline{\psi_{\mathbf{\overline{5}}}^{\alpha}} & \overline{\psi_{\mathbf{10}}^{v}} \end{array} \right) \left(\begin{array}{cc} Y_{d\ell}^{\alpha\beta} \phi_{\mathbf{5}}^{*} & Y_{d\ell}^{\prime\alpha} \phi_{\mathbf{5}}^{*} \\ M_{10}^{\beta} + \lambda_{10}^{\beta} \phi_{\mathbf{24}} & M_{10}^{V} + \lambda_{10}^{V} \phi_{\mathbf{24}} \end{array} \right) \left(\begin{array}{cc} (\psi_{\mathbf{10}}^{\beta})^{c} \\ \psi_{\mathbf{10}}^{v} \end{array} \right) + \text{h.c.}$$

$$\rightarrow \left(\begin{array}{cc} \overline{(D_{R}^{\alpha})^{c}} & \overline{D_{V}^{\prime}} \end{array} \right) \left(\begin{array}{cc} \frac{1}{\sqrt{2}} v_{5} Y_{d\ell}^{\alpha\beta} & \frac{1}{\sqrt{2}} v_{5} Y_{d\ell}^{\prime\alpha} \\ M_{10}^{\beta} + \frac{1}{4} \lambda_{10}^{\beta} v_{24} & M_{10}^{V} + \frac{1}{4} \lambda_{10}^{V} v_{24} \end{array} \right) \left(\begin{array}{c} (D_{L}^{\beta})^{c} \\ D_{V}^{\prime} \end{array} \right) +$$

$$\left(\begin{array}{cc} \overline{E_{L}^{\alpha}} & \overline{E_{V}} \end{array} \right) \left(\begin{array}{c} \frac{1}{\sqrt{2}} v_{5} Y_{d\ell}^{\alpha\beta} & \frac{1}{\sqrt{2}} v_{5} Y_{d\ell}^{\prime\alpha} \\ M_{10}^{\beta} + \frac{3}{2} \lambda_{10}^{b} v_{24} & M_{10}^{V} + \frac{3}{2} \lambda_{10}^{V} v_{24} \end{array} \right) \left(\begin{array}{c} E_{R}^{\beta} \\ E_{V} \end{array} \right),$$

$$(17)$$

where D'_V is the Q = -1/3 state in Q_V .

In this scenario, the states belonging to the vector-like fermions $\psi_{\bf \bar{5}}^v$ or $\psi_{\bf 10}^v$ would also contribute to the running of the gauge couplings, alongside the scalar fields in $\phi_{\bf 5}$ and $\phi_{\bf 15}$, see Table 1.

3 Fit of the mass spectrum of minimal models

In this section, we present the results of a Bayesian analysis aimed at constraining the mass spectrum of the models introduced above. In principle, the physical masses of the new particles displayed in Table 1 could range from m_Z to M_{GUT} (or above). However, the parameter space is tightly constrained because (i) the three SM gauge coupling constants of a realistic GUT model must converge at a high-energy scale, and (ii) such scale must be large enough not to cause unacceptably fast proton decay rates.

Gauge coupling unification. Solving the renormalisation group equations (RGEs) of the SM gauge couplings (taking into account the effect of the new intermediate-scale fields), one can impose the unification of the three constants $\alpha_i \equiv g_i^2/4\pi$ to a common value α_{GUT} at a scale M_{GUT} . At one loop, this provides the three following equations [34]:

$$\alpha_{\text{GUT}}^{-1} = \alpha_i^{-1}(m_Z) - \frac{b_i^{\text{eff}}}{2\pi} \ln\left(\frac{M_{\text{GUT}}}{m_Z}\right), \quad b_i^{\text{eff}} \equiv b_i^{\text{SM}} + \sum_I b_i^I r_I, \quad r_I \equiv \frac{\ln(M_{\text{GUT}}/M_I)}{\ln(M_{\text{GUT}}/m_Z)} \subset [0, 1],$$
 (18)

where i=1,2,3 labels the three gauge interactions, b_i^{SM} are the one-loop β -function coefficients, $(b_3^{\text{SM}}, b_2^{\text{SM}}, b_1^{\text{SM}}) = (-7, -19/6, 41/10)$, due to the SM field content, and the index I runs over the new fields with mass $M_I < M_{\text{GUT}}$, whose contributions to the β functions are denoted as b_i^I . The latter quantities just depend on the quantum numbers of the fields under $SU(3)_c \times SU(2)_L \times U(1)_Y$, see e.g. [35], and are listed in the last three columns of Table 1.

Eliminating α_{GUT} and $\ln(M_{\text{GUT}}/m_Z)$ in Eq. (18), one can get a constraint on the mass spectrum from gauge coupling unification, in terms of experimentally measured quantities [34]:

$$\frac{b_2^{\text{eff}} - b_3^{\text{eff}}}{b_1^{\text{eff}} - b_2^{\text{eff}}} = \frac{\alpha_2^{-1}(m_Z) - \alpha_3^{-1}(m_Z)}{\alpha_1^{-1}(m_Z) - \alpha_2^{-1}(m_Z)} = \frac{5\sin^2\theta_w - 5\alpha_{em}/\alpha_s}{3 - 8\sin^2\theta_w} = 0.717 \pm 0.002,$$
(19)

where $\alpha_{em}^{-1} = 127.952 \pm 0.009$, $\alpha_s \equiv \alpha_3(m_Z) = 0.1179 \pm 0.0009$, $\sin^2 \theta_w = 0.23121 \pm 0.00004$ are, respectively, the electromagnetic coupling constant, the strong coupling constant, and the weak mixing angle at the electroweak scale m_Z [36], and the GUT normalisation $g_1 = \sqrt{5/3} g'$ of the hypercharge coupling has been employed.

For a given set of intermediate fields that satisfy Eq. (19), one can then employ the equations with i = 1, 2 in (18) to obtain the following expression for the GUT scale:

$$\ln\left(\frac{M_{\text{GUT}}}{m_Z}\right) = \frac{6\pi - 16\pi \sin^2\theta_w}{5\alpha_{em}(b_1^{\text{eff}} - b_2^{\text{eff}})}.$$
 (20)

Notice that Eqs. (18-20) neglect the fact that the above-quoted values of b_i^{SM} include the contributions of top quarks, hence it would be correct to consider the running above the top mass scale m_t , that is, to employ $\alpha_i^{-1}(m_t)$ in the formulae and substitute $m_t \to m_Z$ elsewhere. However, the numerical impact would be negligible: using the central values for $\alpha_i^{-1}(m_t)$ calculated in Ref. [28], we find that the quantity in Eq. (19) is shifted to ≈ 0.719 , well within the experimental uncertainty quoted above. Similarly, the effect of the substitution $m_t \to m_Z$ in the logarithms of Eq. (18) is tiny. We expect a larger numerical deviation from the above unification requirement if two-loop RGEs are considered. Such an effect is typically of the same order of magnitude of unknown—in our context—threshold effects from mass splittings of the states at M_I and M_{GUT} (see e.g. the analytical discussion in Ref. [37]). Since, for simplicity, we refrain from modelling the uncertainties due to unknown thresholds, we are going to neglect two-loop corrections as well.

Proton lifetime. As mentioned in the previous section, the extra SU(5) gauge bosons X_{μ} and Y_{μ} can convert quarks and leptons into each other, and thus mediate proton decay.

The current best limits on the proton lifetime were set in 2020 by SuperKamiokande (SK) searching for $p \to \pi^0 e^+$ and $p \to \pi^0 \mu^+$, see Table 2. The contribution of the SU(5) gauge bosons

Mode	Limit (years)	Ref.
$p \to \pi^0 e^+$	$>2.4\times10^{34}$	[38]
$p\to\pi^0\mu^+$	$>1.6\times10^{34}$	[38]
$p \to K^0 e^+$	$> 1.0 \times 10^{33}$	[39]
$p \to K^0 \mu^+$	$>3.6\times10^{33}$	[40]
$p \to \pi^+ \overline{\nu}$	$>3.9\times10^{32}$	[41]
$\underline{\hspace{0.5cm} p \to K^{+} \overline{\nu}}$	$> 5.9 \times 10^{33}$	[42]

Table 2: 90% CL limits from proton decay searches on $\tau(p \to X) \equiv 1/\Gamma(p \to X)$.

to this kind of decay modes (and the analogous ones into neutral kaons) reads [22, 43]

$$\Gamma(p \to \pi^0 \ell_i^+) = \frac{\pi m_p \, \alpha_{\text{GUT}}^2}{2M_{\text{GUT}}^4} A^2 \left\{ \left| (V_1)_{11} (V_3)_{1i} \langle \pi^0 | (ud)_R u_L | p \rangle \right|^2 + \left| \left[(V_1)_{11} (V_2)_{i1} + (V_1 V_{\text{CKM}}^*)_{11} (V_2 V_{\text{CKM}}^T)_{i1} \right] \langle \pi^0 | (ud)_L u_L | p \rangle \right|^2 \right\},$$
(21)

$$\Gamma(p \to K^{0} \ell_{i}^{+}) = \frac{\pi m_{p} \alpha_{\text{GUT}}^{2}}{2M_{\text{GUT}}^{4}} \left(1 - \frac{m_{K}^{2}}{m_{p}}\right)^{2} A^{2} \left\{ \left| (V_{1})_{11}(V_{3})_{2i} \langle K^{0} | (us)_{R} u_{L} | p \rangle \right|^{2} + \left| \left[(V_{1})_{11}(V_{2})_{i2} + (V_{1}V_{\text{CKM}}^{*})_{12}(V_{2}V_{\text{CKM}}^{T})_{i1} \right] \langle K^{0} | (us)_{L} u_{L} | p \rangle \right|^{2} \right\},$$
(22)

where we identified the mass of the mediators X_{μ} and Y_{μ} with M_{GUT} and A is a renormalisation factor accounting for the running of the baryon-number violating operators from the GUT scale to m_p (cf. Appendix B for details and for the numerical values of the hadronic matrix elements). Furthermore, V_{CKM} is the CKM mixing matrix and the other matrices are defined in terms of the biunitary rotations that diagonalise the fermion masses $(V_f^{\dagger}M_fV_f'=M_f^{\text{diag}})$ as follows

$$V_1 \equiv V_u^{\prime\dagger} V_u^* , \quad V_2 \equiv V_\ell^{\prime\dagger} V_d^* , \quad V_3 \equiv V_\ell^{\dagger} V_d^{\prime*} . \tag{23}$$

Within minimal SU(5), all the above matrices equal 1 and the decay width in Eq. (21) only depends on known CKM angles. This is not anymore the case in presence of the more general mass matrices considered in the previous section that can correctly account for the observed fermion mass relations. Thus, in the models we are considering, $p \to \pi^0 \ell_i^+$ depends on the unknown (and, within the SM, unobservable) right-handed rotations V_f' through the combinations in Eq. (23). It is therefore possible that non-trivial (and somewhat tuned) flavour structures of M_f conspire to suppress the p-decay rates in these channels [43, 44].

On the other hand, the decay modes involving neutrinos are subject to weaker constraints (cf. Table 2) but are theoretically more robust. In fact, it has been noted that summing over the (experimentally unobservable) anti-neutrino flavours makes the dependence on the PMNS mixing drop and leads to a much cleaner theoretical prediction for these channels than for $p \to \pi^0 \ell_i^+$ [22, 44]:

$$\Gamma(p \to \pi^{+} \overline{\nu}) = \frac{\pi m_{p} \alpha_{\text{GUT}}^{2}}{2M_{\text{GUT}}^{4}} A^{2} |(V_{1} V_{\text{CKM}})_{11} \langle \pi^{+} | (du)_{R} d_{L} | p \rangle|^{2}, \qquad (24)$$

$$\Gamma(p \to K^{+} \overline{\nu}) = \frac{\pi m_{p} \alpha_{\text{GUT}}^{2}}{2M_{\text{GUT}}^{4}} \left(1 - \frac{m_{K}^{2}}{m_{p}}\right)^{2} A^{2} \left\{ \left| (V_{1} V_{\text{CKM}})_{11} \langle K^{+} | (us)_{R} d_{L} | p \rangle \right|^{2} + \left| (V_{1} V_{\text{CKM}})_{12} \langle K^{+} | (ud)_{R} s_{L} | p \rangle \right|^{2} \right\}.$$
(25)

As we can see, the only residual dependence on the fermion flavour structure is encoded in V_1 , a matrix that equals the identity if the up-quark mass matrix M_u is symmetric. In our models, this occurs if the contribution $\propto Y_u''$ is subdominant in Eq. (8) (Model 1), that $\propto Y_u'$ is negligible in Eq. (13) (Model 2), and only $\mathbf{5} + \mathbf{\bar{5}}$ vector-like fermions are introduced (Model 3). Furthermore, even for a non-symmetric M_u , the results obtained setting $V_1 \to \mathbb{1}$ in Eqs. (24, 25) are still a very good approximation if V_u' has got a hierarchical structure akin to that observed in the left-handed sector.

Finally, let us notice that, besides the vector bosons X_{μ} and Y_{μ} , scalar particles such as the colour triplet in $\phi_{\bf 5}$ and φ_3^T , φ_3^S , φ_3^S (cf. Table 1) also endanger proton stability.⁵ When considering minimal scenarios, it is therefore reasonable to set their masses at the GUT scale directly. However, when the relevant Yukawa couplings are small, these fields could also be lighter than M_{GUT} by several orders of magnitude. We will comment about their possible impact on our fit below.

 $^{^5}$ Our scalar fields could induce both B-L conserving and violating processes, see Appendix $^{\rm B}$ for details.

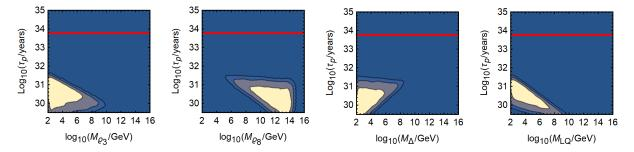


Figure 1: Result of the fit for Model 1 (non-renormalisable operators) shown on planes displaying the extra field masses and the proton lifetime from $p \to K^+ \bar{\nu}$ (the most constraining of the theoretically clean decay modes). The red line depicts the corresponding SK lower limit, 5.9×10^{33} years [42]. Regions favoured by the fit at 1σ , 2σ and 3σ are highlighted.

Fitting procedure. The mass spectrum is calculated by means of the following steps. Firstly, we sample uniformly the initial parameters in Eq. (18), $\{r_I \subset [0,1]\}$, and enforce the unification constraint of Eq. (19). Next, we calculate the resulting GUT scale according to Eq. (20), and use it in Eq. (18) to obtain the masses of the new particles, $\{M_I\}$, and the unified coupling α_{GUT} . This information can be converted into a prediction for the proton decay rates, once additional assumptions on the flavour structure of the mixing in Eq. (23) are made (that we will discuss below, when presenting our results). Finally, applying the relevant SK bounds on proton decay reported in Table 2, we get probability distributions for the spectrum of the new particles and the proton lifetime.

We start considering the simplest models (that is, minimal in terms of field content) that are compatible with all phenomenological observations related to neutrino and fermion masses and proton stability, thus reducing the number of free parameters in our fit. First, let us notice that the particles whose contribution to the $U(1)_Y$ β -function coefficient is larger than the $SU(2)_L$ one should better not contribute much to the running of the gauge couplings, as their effect is to decrease $M_{\rm GUT}$ and thus endanger proton stability (according to Eq. (20), $(b_1^{\rm eff} - b_2^{\rm eff})$ should be as small as possible for the sake of a large $M_{\rm GUT}$). Therefore, we start setting the masses of such fields at $M_{\rm GUT}$. Similarly, we do not consider at first scalars that directly mediate proton decay, as we mentioned above. Under these assumptions, our parameter space is rather limited; we will discuss below how the fit is affected by enlarging it. All models have as free parameters the masses of the $SU(2)_L$ triplet ϱ_3 and the colour octet ϱ_8 from the GUT Higgs 24, and those of the seesaw triplet Δ and the leptoquark \widetilde{R}_2 from the 15, cf. Table 1. In addition, Model 2 features the masses of the colour octet and the second Higgs doublet in the 45, φ_8 and H_2 , and Model 3 the vector-like fermions $L_V + L_V^c$ and $Q_V + Q_V^c$.

3.1 Model 1

As discussed above, the minimal setup of this model just comprises 4 parameters. In Figure 1, we show the result of the fit in terms of these parameters and the resulting proton lifetime. The latter was estimated based only on the theoretically clean mode $p \to K^+ \overline{\nu}$, assuming that $p \to \pi^0 \ell_i^+$ can be somewhat suppressed by the flavour structure of the fermion masses. For the calculation, we have taken for the mixing matrix $V_1 = 1$, cf. Eq. (23), hence the plots illustrate to a very good approximation both the case of an (approximately) symmetric up-quark mass matrix, as well as a hierarchical structure of the right-handed mixing. For this fit, we did not impose the experimental proton decay limits. In fact, as we can see, the region favoured by the fit corresponds to a proton lifetime more than two orders of magnitude smaller than the present SK bound. Therefore, this setup is excluded, barring very fine-tuned flavour structures of that Yukawa matrices such that $p \to \pi^0 \ell_i^+$, $p \to \pi^+ \overline{\nu}$, and $p \to K^+ \overline{\nu}$ be all simultaneously suppressed.

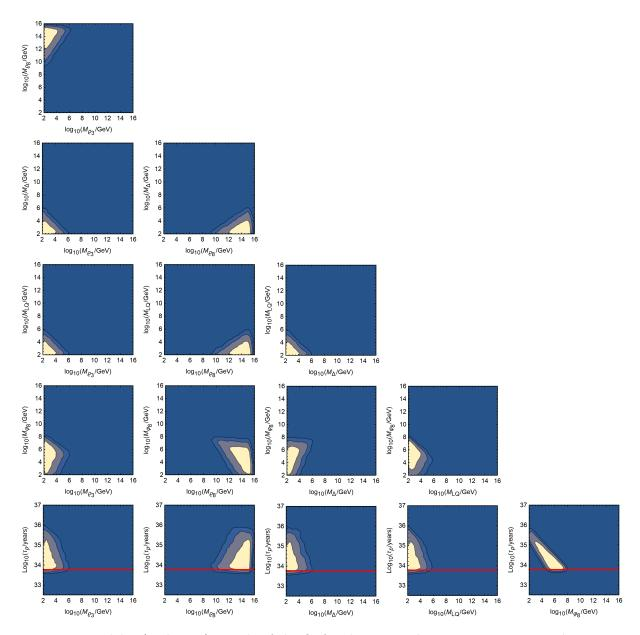


Figure 2: Model 2 (scalar 45): result of the fit for the minimal 6-parameter setup. The proton lifetime τ_p vs. the mass parameters and the two-dimensional correlation plots for the particle masses are shown. τ_p was calculated considering the clean $p \to K^+ + \overline{\nu}$ decay modes. Colours as in Figure 1.

The reason why this model is so strongly disfavoured is that there are too few parameters to achieve a high M_{GUT} . Enlarging the parameter space by including more states from ϕ_{24} and ϕ_{15} with $M_I < M_{\text{GUT}}$ would not improve the situation: as discussed above, the presence of these other fields would, in fact, tend to further lower M_{GUT} and/or introduce new sources of p decay.

3.2 Model 2

In Model 2, we have in addition φ_8 and H_2 (both from ϕ_{45}) that, as argued above, can contribute to gauge coupling unification without endangering proton stability. We start considering only the effect of the colour octet and $SU(2)_L$ doublet φ_8 —alongside the fields contained in ϕ_{24} and ϕ_{15} that we included in the fit of Model 1—while set the mass of the second Higgs doublet H_2 equal to M_{GUT} . The outcome of this 5-parameter fit is shown in Figure 2. As for Model 1,

proton lifetime was calculated considering $p \to K^+ \overline{\nu}$ with $V_1 = 1$ and conservatively assuming that flavour mixing can suppress $p \to \pi^0 \ell_i^+$ to a sufficient extent. Here, in contrast to Model 1, we are imposing the SK bound as a constraint of the fit. As we can see from the last row of Figure 2, the effect of the colour octet φ_8 is to raise the GUT scale to such an extent that, at the $1\sigma(3\sigma)$ level, a proton lifetime up to about $10^{35}(36)$ years can be easily achieved. This requires the octet to live at an intermediate to low scale ($\lesssim 10^8$ GeV). In fact, the proton lifetime is anti-correlated to the octet mass (cf. the bottom-right plot of the figure), as first observed in Ref. [12]. The plots in Figure 2 also show that a good fit requires that the Y = 0 triplet ϱ_3 from φ_{24} as well as the seesaw triplet Δ and the scalar leptoquark R_2 from φ_{15} should all be rather light ($\lesssim 10$ TeV, at 1σ).

This scenario could be regarded as a 'minimal predictive grand-unified type II seesaw model'. Indeed, it is 'minimal' and 'predictive' due to the following reasons:

- Only bosonic fields are added to the SM (and to minimal SU(5)), no additional (vector-like) fermions are required. Furthermore, both the scalar **15** and **45** representations are contained in a single SO(10) representation of dimension **126**.
- All of the 5 new particles considered in Figure 2 are necessary for a successful gauge coupling unification. As shown below, φ_8 can not be replaced with H_2 as the latter field does not raise M_{GUT} so much. In addition, even the 'scalar gluon' ϱ_8 , which does not contribute to the running of $\alpha_{1,2}$, is also crucial, because it can help balance $(b_2^{\text{eff}} b_3^{\text{eff}})$ and $(b_1^{\text{eff}} b_2^{\text{eff}})$ in Eq. (19), when the latter quantity increases.
- No fine tuning in the Yukawa sector is required and all the flavour mixing angles could have 'natural' and generic values.
- As we have seen, light fields are predicted, in particular the weak triplet Δ and the leptoquark $\widetilde{R_2}$, which could therefore induce large LFV effects, as we are going to discuss in the next section.
- The Y=0 triplet ϱ_3 is also required to be light. Interestingly, this field can be responsible for the shift of the W boson mass that the recent result of the CDF collaboration [45] seems to indicate: the anomaly can be accommodated with $M_{\varrho_3} \approx 10$ TeV if the triplet-Higgs doublet trilinear coupling (in our context $\phi_5\phi_5\phi_{24}$) is of order M_{ϱ_3} [46].
- The anti-correlation between the mass of the octet φ_8 and the proton lifetime has important phenomenological implications: if proton decay will be further constrained by next-generation large-volume detectors, such as JUNO [49], DUNE [50], Hyper-Kamiokande [51], φ_8 could be an accessible target for future runs of the LHC or the proposed high-energy hadron colliders. Vice versa, if colliders further constrain the φ_8 mass, this would favour a proton lifetime possibly within the reach of future experiments.

As the above-discussed 'minimal grand-unified type II seesaw model' has so many interesting phenomenological implications, it is important to discuss how robust the latter are. In other words, if we introduce more parameters, will the favoured masses of LFV mediators and the $M_{\varphi_8} - \tau_p$ correlation change much? We can consider three paths for a next-to-minimal extension of the minimal scenario:

(1) Set all the other particles (S from ϕ_{15} and $\varphi_{\overline{6}}$, φ_3^D , H_2 from ϕ_{45}) except for the proton decay mediators lighter than the GUT scale, such that they can also contribute to the RGEs. Due to the presence of the second Higgs doublet—the only among these fields that, as argued above, can have a positive impact on gauge coupling unification—we label this scenario 2HDM (two Higgs doublet model).

⁶ For discussions of the CDF anomaly with a Y=0 triplet in the context of GUTs see [47, 48].

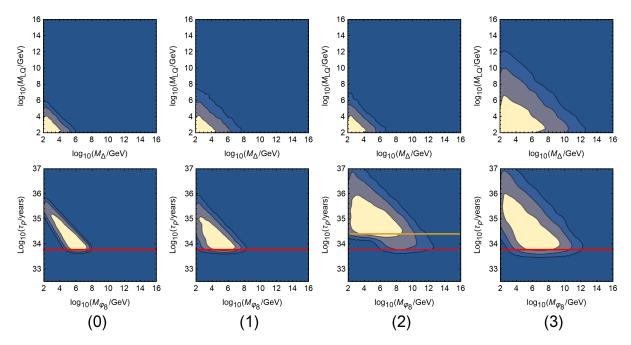


Figure 3: Impact on M_{Δ} , M_{LQ} , and the $M_{\varphi_8} - \tau_p$ correlation of relaxing the assumptions of the Model 2 fit. From left to right: (0) minimal setup as in Figure 2, (1) 2HDM, (2) generic flavour mixing, (3) p-decay mediators. See the text for details.

- (2) Allow arbitrary flavour mixing, that is, include the mixing angles in the matrices (23) among the free parameters to fit.⁷ This may suppress proton decay rates and relax the mass constraints on the light particles. In fact, according to Eq. (10), M_u receives an anti-symmetric contribution such that V_1 is now a general unitary matrix.
- (3) Take the scalar proton decay mediators (the colour triplet H_T in ϕ_5 , the ϕ_{45} fields φ_3^T , ϕ_{45} and φ_3^S) lighter than M_{GUT} . We let their masses free to range from M_{GUT} down to about 10^{13} GeV, which is the order of magnitude of the bounds from p-decay searches if the values of the couplings of these fields to SM fermions are in the ballpark of the SM Yukawa couplings [43].

Figure 3 and Table 3 show the impact on the fit of the above relaxed assumptions. While the 3σ upper bounds soar in the next-to-minimal scenarios, the 1σ -favoured regions remain at the TeV scale, with the exception of case (3), where the fit is substantially relaxed. In fact, among all these new scalars, only φ_3^T and H_2 from φ_{45} satisfy $b_1^I < b_2^I$ and thus can play a role in relaxing the mass bounds in the next-to-minimal scenarios, while the other fields considered in scenarios (1) and (3) can only decrease M_{GUT} and thus in fact tighten these mass bounds. Similarly, relaxing the flavour structure of the fermion mass matrices can loosen the p-decay constraints and have a significant impact on the $M_{\varphi_8} - \tau_p$ correlation (cf. the column (2) of Figure 3 where we plot $\min[\tau(p \to \pi^0 e^+), \tau(p \to K^+ \overline{\nu})]$ and show both experimental limits) but does not affect much the prediction for the masses of the seesaw triplet and the leptoquark.

Searches for the production of new-physics particles at the LHC have already started to test this model. Constraints on the mass of Δ can be obtained searching, in particular, for the electroweak production of the doubly-charged states $pp \to \Delta^{++}\Delta^{--}$ followed by decays into same-sign leptons or W bosons, $\Delta^{++} \to \ell_i^+ \ell_j^+$ and $\Delta^{++} \to W^+ W^+$. The former mode—which

⁷In this case, we can impose the bounds from all the proton decay channels, $p \to \pi^0/K^0 + e^+/\mu^+$ and $p \to \pi^+/K^+ + \overline{\nu}$, as we have all information to calculate the rates in Eqs. (21-25).

⁸The impact of H_2 is however very mild, as shown by the results for case (1) in Figure 3 and Table 3. Notice in particular that a light φ_8 is still required to achieve successful unification.

(0) minimal fit	M_{Δ} (TeV)	M_{LQ} (TeV)
1σ UL	1.6	1.5
2σ UL	39	33
3σ UL	449	335
(1) 2HDM	M_{Δ} (TeV)	M_{LQ} (TeV)
1σ UL	2.2	1.6
2σ UL	136	73
3σ UL	6.4×10^3	4.8×10^{3}
(2) flavour mix.	M_{Δ} (TeV)	M_{LQ} (TeV)
1σ UL	2.0	1.5
2σ UL	61	48
3σ UL	1.6×10^3	1.5×10^3
(3) p -decay med.	M_{Δ} (TeV)	M_{LQ} (TeV)
1σ UL	134	33
2σ UL	1.5×10^5	4.9×10^4
	1.8×10^{8}	8.5×10^{7}

Table 3: Model 2: 1σ , 2σ , and 3σ upper limits (UL) of the marginalised 1D probability distributions of the masses of the ϕ_{15} fields Δ and \widetilde{R}_2 for the minimal setup and the next-to-minimal fits described in the main text.

dominates if the vev of Δ induced by electroweak symmetry breaking is small, $\langle \Delta \rangle \lesssim 10^{-4}$ GeV, see e.g. [52] — provides a cleaner signature that leads to a stronger limit, $M_{\Delta} \gtrsim 800$ GeV [53]. If on the contrary the decay into W dominates, the current lower limit on M_{Δ} is about 350 GeV [54].

Bounds on leptoquarks are even more stringent, as \widetilde{R}_2 can be copiously produced via strong interactions. The state with Q=2/3 decays fully visibly into (right-handed) down-type quarks and charged leptons, $\widetilde{R}_2^{2/3} \to \ell_i^+ d_j$. As we will discuss in the next section, the flavour structure of the \widetilde{R}_2 couplings (like that of Δ) is dictated by the neutrino mass matrix, that is, by the large PMNS mixing angles. Therefore, \widetilde{R}_2 tends to decay 'democratically' into all combinations of quark and lepton flavours, resulting in a large yield for the signal e/μ +jet and a limit $M_{LQ} \gtrsim 1.6 - 1.8$ TeV [55].

The phenomenology of the colour-octet isospin doublet ϱ_8 has been extensively studied in the context of minimal extensions of the SM scalar sector, starting from Ref. [56]. After production via strong interactions, both states in ϱ_8 (charged and neutral) would decay into quark pairs through the couplings Y'_u and $Y'_{d\ell}$ in Eq. (10). If these matrices feature a flavour hierarchy resembling that of the SM Yukawa couplings, decays into third generation quarks ($\varrho_8^0 \to t\bar{t}$, $\varrho_8^+ \to t\bar{b}$) will dominate. In such a case, the current LHC bounds are estimated to be in the 800–1000 GeV range [57–59]. However, notice that only sizeable couplings to first and second generation down-type quarks are strictly required in order to correct the relations in Eq. (5). If such couplings dominate, the particles in the octet would mostly decay into two light jets and, thus, be subject to much more stringent constraints from searches for heavy di-jet resonances, corresponding to a lower bound of about 4 TeV [60].

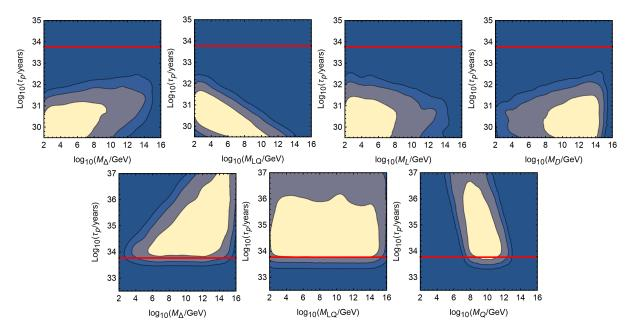


Figure 4: Results of the fit for Model 3, considering the minimal field content of Figure 1 plus one generation of vector-like fermions in the $\mathbf{5} + \overline{\mathbf{5}}$ representation (first row) or one generation in the $\mathbf{10} + \overline{\mathbf{10}}$ (second row).

3.3 Model 3

In the case of Model 3, where only vector-like fermions are added to the minimal SU(5) field content, the regions of the parameter space favoured by the fit are very different. As discussed above, correct fermion mass relations and unification can be achieved by the usual fields in ϕ_{24} and ϕ_{15} plus vector-like leptons $L_V + L_V^c$ (that is, introducing a fermionic $\mathbf{5} + \overline{\mathbf{5}}$), but the impact of these latter field on M_{GUT} is limited. As a consequence, one generation of vector-like leptons is far insufficient to raise M_{GUT} with respect to Model 1 (Figure 1) at a level compatible with the p-decay bounds. This is shown in the first row of Figure 4. Only multiple $5+\bar{5}$ generations could evade the limits on p-decay without relying on tuning in the fermion mixing. We checked that at least five generations are needed. On the other hand, if one introduces fermions in the $10 + \overline{10}$, only one generation of $Q_V + Q_V^c$ is enough to achieve unification at a large enough M_{GUT} . In the latter case, the ϕ_{15} fields Δ and R_2 do not even need to be light. This is explicitly shown in the second row of Figure 4. As we can see, the central values for M_{Δ} and M_{LQ} could be much higher compared to the results we shown for Model 2 (cf. Table 3) and their 1σ favoured ranges span almost all scales between m_Z and M_{GUT} . Hence Model 3 (with a single $10 + \overline{10}$), while being perfectly viable, completely lacks the predictivity and the interesting phenomenological features of Model 2. A similar conclusion would hold also for the case of multiple (≥ 5) $5 + \bar{5}$ generations, as shown by the first row of Figure 4.

4 Type II seesaw fields and Lepton Flavour Violation

In this section, we focus on the low-energy phenomenology of the fields in ϕ_{15} associated to the generation of neutrino masses. In particular, the seesaw triplet Δ and the scalar leptoquark \widetilde{R}_2 unavoidably mediate LFV interactions, as we are discussing in the following. Furthermore, within the most successful (and predictive) of the models analysed above (see Section 3.2), gauge coupling unification requires them to be rather light, $\lesssim \mathcal{O}(10)$ TeV, which makes searches for LFV processes the most promising experimental handle to test type II seesaw unification.

The couplings to leptons of these fields follow from the third term in Eq. (4):

$$-\mathcal{L}_{\text{Yukawa}} \supset Y_{15}^{\alpha\beta} \, \overline{\psi_{\overline{5}}}_{\alpha} \phi_{15}^* \psi_{\overline{5}\beta}^c + \text{h.c.} \rightarrow Y_{\Delta}^{\alpha\beta} \, \overline{L_L}_{\alpha} \Delta i \sigma_2 L_{L\beta}^c + Y_{LQ}^{\alpha\beta} \, \overline{D_R}_{\alpha} \widetilde{R_2} L_{L\beta} + \text{h.c.}, \quad (26)$$

where α and β are flavour indices and we work in the basis where the charged-lepton and downquark mass matrices are flavour diagonal. The conventions we adopt for the decomposition of the $SU(2)_L$ representations are

$$\Delta = \begin{pmatrix} \Delta^{-}/\sqrt{2} & \Delta^{0} \\ \Delta^{--} & -\Delta^{-}/\sqrt{2} \end{pmatrix}, \qquad \widetilde{R_{2}}^{T} = \left(\widetilde{R_{2}}^{2/3}, \widetilde{R_{2}}^{-1/3}\right). \tag{27}$$

At the GUT scale the triplet and leptoquark Yukawa matrices in Eq. (26) match to Y_{15} as

$$Y_{\Delta} = Y_{LQ}/\sqrt{2} = Y_{15}$$
, [GUT scale]. (28)

At lower scales, they are renormalised according to the RGEs reported in Appendix C, resulting in the TeV-scale relation

$$Y_{LQ} \approx 2.1 \, Y_{\Delta} \,, \qquad \text{[TeV scale]} \,.$$
 (29)

What makes this framework predictive is that the flavour structure of both matrices is related to the observed neutrino masses and mixing. Neutrino mass terms arise from the explicit breaking of the lepton number that is a consequence of the couplings of the triplet to leptons in Eq. (26) in combination with the following scalar potential term:

$$-\mathcal{L} \supset \mu \phi_{\mathbf{5}} \phi_{\mathbf{15}}^* \phi_{\mathbf{5}} + \text{h.c.} \rightarrow \mu_{\Delta} H^T i \sigma_2 \Delta H + \text{h.c.}.$$
 (30)

The resulting Majorana neutrino mass matrix reads

$$m_{\nu} = \sqrt{2} Y_{\Delta} v_{\Delta} = Y_{\Delta} \frac{\mu_{\Delta} v^2}{M_{\Delta}^2},$$
 (31)

where v_{Δ} is the vev the triplet acquires upon electroweak symmetry breaking, that is, $\langle \Delta^0 \rangle = v_{\Delta}/\sqrt{2}$, and $v = v_5$. Eq. (31) shows that the flavour structure of the matrix Y_{Δ} —and consequently of Y_{LQ} too—is the same as that of the neutrino mass matrix. In other words, in the charged-lepton mass basis, Y_{Δ} unavoidably features off-diagonal LFV entries dictated by the (large) mixing angles of the PMNS matrix, following from

$$m_{\nu}^{\text{diag}} = U_{\text{PMNS}}^T m_{\nu} U_{\text{PMNS}}, \qquad (32)$$

where m_{ν}^{diag} is the diagonal matrix of the neutrino mass eigenvalues (m_1, m_2, m_3) and U_{PMNS} is the PMNS mixing matrix (cf. Appendix D for details). Notice however that the absolute size of the couplings in Y_{Δ} and Y_{LQ} is not uniquely determined (even for a given M_{Δ}) because of the dependence of m_{ν} on the lepton-breaking dimensionful parameter μ_{Δ} . In particular, for a small enough μ_{Δ} , the observed values of the neutrino masses can be reproduced even with a light triplet and $\sim \mathcal{O}(1)$ couplings in Y_{Δ} —which greatly enhances the LFV effects, as we will show below. On the other hand, the Yukawa couplings could still be extremely small if μ_{Δ} is sizeable. Ratios of rates of different LFV processes overcome this source of uncertainty and, as discussed below, can provide further constraints on the spectrum of the model, in particular on the ratio M_{LQ}/M_{Δ} . This opportunity, in combination with the unification requirements on the particle masses and the fact that, following from Eq. (26), the leptoquark couplings Y_{LQ} are flavour symmetric and linked to the neutrino mass matrix, makes the LFV phenomenology of SU(5) type-II seesaw models much more predictive than the generic setups previously studied, e.g. in the model-independent analyses of Refs. [4, 27].

⁹This is equal to $v_{\rm EW} \approx 246$ GeV for models without a second Higgs doublet. On the contrary, if $H_2 \subset \phi_{45}$ exists, one has $v_5 = v_{\rm EW} \cos \beta$ with $\tan \beta \equiv v_{45}/v_5$ being a free parameter. If this is the case, the bounds on the couplings discussed below have to be rescaled by an $\mathcal{O}(1)$ factor, while the rest of the phenomenological discussion does not change.

¹⁰One can obtain the loose lower bound $|Y_{\Delta}^{\alpha\beta}| \gtrsim 10^{-12}$ from the electroweak-fit constraint on $\Delta\rho$, which requires $v_{\Delta} \lesssim 1$ GeV (see e.g. [61]) in Eq. (31).

Observable	90% CL upper limit	Future sensitivity
$BR(\mu^+ \to e^+ \gamma)$	$4.2 \times 10^{-13} [62]$	$6 \times 10^{-14} [63]$
${\rm BR}(\mu^+\to e^+e^-e^+)$	$1.0 \times 10^{-12} [64]$	$10^{-16} [65]$
$CR(\mu^- N \to e^- N)$	$7.0 \times 10^{-13} \ (N = \text{Au}) \ [66]$	$6 \times 10^{-17} \ (N = \text{Al}) \ [67, 68]$
$\overline{\mathrm{BR}(K_L \to \mu^{\pm} e^{\mp})}$	4.7×10^{-12} [69]	$\sim 10^{-12} [70]$
$\mathrm{BR}(K_L \to \pi^0 \mu^+ e^-)$	7.6×10^{-11} [71]	$\sim 10^{-12} \ [70]$
${\rm BR}(K^+\to\pi^+\mu^+e^-)$	$1.3 \times 10^{-11} $ [72]	$\sim 10^{-12} \ [70]$
$BR(K^+ \to \pi^+ \mu^- e^+)$	$5.2 \times 10^{-10} $ [73]	$\sim 10^{-12} [70]$

Table 4: Current experimental bounds and future expected sensitivities on the LFV processes relevant for our analysis.

4.1 LFV observables

Both the triplet Δ and the leptoquark $\widetilde{R_2}$ induce LFV processes already at the tree level. Here we focus on $\mu - e$ flavour violation that is subject to the best limits at present and has the most promising experimental prospects, see e.g. [24]. Present bounds and future expected sensitivities on the processes we are interested in are reported in Table 4.

A tree-level exchange of the triplet mediates $\mu \to eee$ [4]:

$$BR(\mu \to eee) = \frac{1}{4G_F^2 M_\Delta^4} |Y_\Delta^{21}|^2 |Y_\Delta^{11}|^2$$
 (33)

where G_F is the Fermi constant.

The leptoquark R_2 can induce at tree level $\mu \to e$ conversion in atomic nuclei, with a conversion rate given by [15, 27]:

$$CR(\mu N \to e N) = \frac{m_{\mu}^{5}}{4\Gamma_{\text{capt}} M_{LQ}^{4}} \left(V^{(p)} + 2V^{(n)}\right)^{2} \left|Y_{LQ}^{21}\right|^{2} \left|Y_{LQ}^{11}\right|^{2}, \tag{34}$$

which is as usual normalised by the capture rate Γ_{capt} of muons by the nucleus N. $V^{(p)}$ and $V^{(n)}$ are overlap integrals between muon and electron wave functions and nucleons density distributions [74]. The most recent evaluation of these quantities can be found in Ref. [75].

The leptoquark also contributes at tree level to LFV decays of mesons, in particular the tightly constrained neutral kaon decay $K_L \to \mu e$, whose branching ratio reads [15, 27]:

$$BR(K_L \to \mu e) = \frac{m_K \tau_{K_L}}{256\pi} \frac{m_\mu^2 f_{K_L}^2}{M_{LQ}^4} \left(1 - \frac{m_\mu^2}{m_{K_L}^2} \right)^2 \left| Y_{LQ}^{12} Y_{LQ}^{12*} + Y_{LQ}^{11} Y_{LQ}^{22*} \right|^2, \tag{35}$$

where $f_{K_L} \simeq 160$ MeV and $\tau_{K_L} = 5.116 \times 10^{-8}$ s are K_L decay constant and lifetime [36]. Semileptonic kaon decays are also induced. Following [76], we find

$$\frac{d}{dq^2} BR(K \to \pi \mu e) = \frac{(m_{\mu}^2 - q^2)^2 \tau_K \lambda^{\frac{1}{2}} (\sqrt{q^2}, m_K, m_{\pi})}{12288 \pi^3 m_K^3 M_{LQ}^4 q^6} \mathcal{Y}
\times \left[3|f_0(q^2)|^2 (m_K^2 - m_{\pi}^2)^2 m_{\mu}^2 + |f_+(q^2)|^2 (m_{\mu}^2 + 2q^2) \lambda(\sqrt{q^2}, m_K, m_{\pi}) \right],$$
(36)

¹¹The present best limit on $\mu \to e$ conversion was obtained on gold and the upcoming experiments plan to employ aluminium targets, see Table 4. Thus we are using the following input for our analysis [75]: $V^{(p)}(\mathrm{Au}) = 0.0866$, $V^{(n)}(\mathrm{Au}) = 0.129$ and $\Gamma_{\mathrm{capt}}(\mathrm{Au}) = 13.07 \times 10^6 \, \mathrm{s}^{-1}$; $V^{(p)}(\mathrm{Al}) = 0.0165$, $V^{(n)}(\mathrm{Al}) = 0.0178$ and $\Gamma_{\mathrm{capt}}(\mathrm{Al}) = 0.7054 \times 10^6 \, \mathrm{s}^{-1}$. The capture rates were taken from [74].

where $q^2 = (p_{\mu} + p_e)^2$ (with $m_{\mu}^2 \lesssim q^2 \leq (m_K - m_{\pi})^2$), $\lambda(a, b, c) \equiv [a^2 - (b - c)^2][a^2 - (b + c)^2]$, and the form factors are about the same for K^+ and K_L (up to percent level corrections [77]) and depend very weakly on q^2 [78]. For our numerical study, we employ $f_0(q^2) \simeq f_+(q^2) \simeq f_0(0) \simeq f_+(0) \simeq 0.9677$ [79]. The above expression depends on the following combinations of couplings:

$$\mathcal{Y} = \begin{cases}
|Y_{LQ}^{12}|^4 & [K^+ \to \pi^+ \mu^+ e^-], \\
|Y_{LQ}^{11} Y_{LQ}^{22*}|^2 & [K^+ \to \pi^+ \mu^- e^+], \\
\frac{1}{2} |Y_{LQ}^{12} Y_{LQ}^{12*} + Y_{LQ}^{11} Y_{LQ}^{22*}|^2 & [K_L \to \pi^0 \mu^+ e^-].
\end{cases}$$
(37)

As one can see from Eq. (35), $K_L \to \pi^0 \mu^+ e^-$ has the same dependence as $K_L \to \mu e$, and one numerically finds $\mathrm{BR}(K_L \to \pi^0 \mu^+ e^-) \approx 0.04 \times \mathrm{BR}(K_L \to \mu^+ e^-)$, hence it can not provide additional information. On the contrary, both $K^+ \to \pi^+ \mu^+ e^-$ and $K^+ \to \pi^+ \mu^- e^+$ have a cleaner dependence on the entries of Y_{LQ} , hence they can help to study its flavour structure, as we will see below.

In principle, both the triplet and the leptoquark also induce $\mu \to e\gamma$ at one loop. However, the contribution from loops involving down-type quarks and \widetilde{R}_2 is strongly suppressed—the terms in the amplitude being $\propto (m_{d,s,b}/M_{LQ})^2$ —thus the branching ratio is very well approximated by the contribution of the type II seesaw triplet alone [4]:

$$BR(\mu \to e\gamma) = \frac{\alpha}{48\pi G_F^2 M_{\Delta}^4} \frac{25}{64} \left| \sum_{\beta} Y_{\Delta}^{2\beta} * Y_{\Delta}^{1\beta} \right|^2.$$
 (38)

4.2 Numerical analysis

Numerically, the above formulae give

$$BR(\mu \to eee) \simeq 1.1 \times 10^{-12} \left(\frac{10 \text{ TeV}}{M_{\Delta}} \right)^{4} \left(\frac{|Y_{\Delta}^{21}|^{2} |Y_{\Delta}^{11}|^{2}}{0.05^{4}} \right),$$

$$BR(\mu \to e\gamma) \simeq 3.6 \times 10^{-13} \left(\frac{10 \text{ TeV}}{M_{\Delta}} \right)^{4} \left(\frac{\left|\sum_{\beta} Y_{\Delta}^{2\beta} * Y_{\Delta}^{1\beta}\right|^{2}}{0.4^{4}} \right),$$

$$CR(\mu \text{ Au} \to e \text{ Au}) \simeq 2.4 \times CR(\mu \text{ Al} \to e \text{ Al}) \simeq 7.3 \times 10^{-13} \left(\frac{10 \text{ TeV}}{M_{LQ}} \right)^{4} \left(\frac{\left|Y_{LQ}^{21}\right|^{2} \left|Y_{LQ}^{11}\right|^{2}}{0.02^{4}} \right),$$

$$BR(K_{L} \to \mu e) \simeq 3.2 \times 10^{-12} \left(\frac{10 \text{ TeV}}{M_{LQ}} \right)^{4} \left(\frac{\left|Y_{LQ}^{12}Y_{LQ}^{12*} + Y_{LQ}^{11}Y_{LQ}^{22*}\right|^{2}}{0.04^{4}} \right),$$

$$BR(K^{+} \to \pi^{+}\mu^{+}e^{-}) \simeq 1.2 \times 10^{-11} \left(\frac{10 \text{ TeV}}{M_{LQ}} \right)^{4} \left(\frac{\left|Y_{LQ}^{21}\right|^{4}}{0.15^{4}} \right),$$

$$BR(K^{+} \to \pi^{+}\mu^{-}e^{+}) \simeq 6.2 \times 10^{-10} \left(\frac{10 \text{ TeV}}{M_{LQ}} \right)^{4} \left(\frac{\left|Y_{LQ}^{11}Y_{LQ}^{22*}\right|^{2}}{0.4^{4}} \right).$$

$$(39)$$

These results, in combination with the experimental limits in Table 4, show that for the spectrum favoured by our Model 2 fit in Section 3.2 (M_{Δ} , $M_{LQ} \lesssim 10$ TeV) the relevant couplings are approximately constrained to be $|Y_{\Delta}^{\alpha\beta}| \lesssim 0.05$, $|Y_{LQ}^{\alpha\beta}| \lesssim 0.02$, with $\mu \to eee$ and $\mu N \to e N$

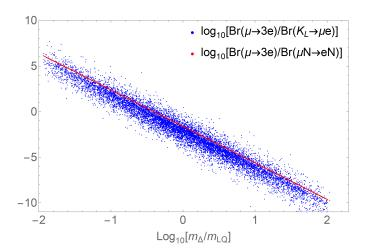


Figure 5: Ratios BR($\mu \to eee$)/CR(μ Al $\to e$ Al) (red points) and BR($\mu \to eee$)/BR($K_L \to \mu e$) (blue points) as functions of M_{Δ}/M_{LQ} . See the text for details.

providing the most stringent bounds, which translate into lower limits on the masses as stringent as $M_{\Delta} \gtrsim 200$ TeV, $M_{LQ} \gtrsim 500$ TeV, for $\mathcal{O}(1)$ couplings. Table 4 and Eq. (39) show that upcoming experiments will improve these limits by about one order of magnitude.

Even if not so constraining, $\mu \to e\gamma$, $K_L \to \mu e$ and $K^+ \to \pi^+ \mu e$ depend on different combinations of the couplings, hence ratios of the branching ratios of different modes can provide information on the flavour structure of Y_{Δ} and Y_{LQ} , that is, on the flavour structure of the neutrino mass matrix, Eq. (31), as we will discuss below.

The matrices Y_{Δ} and Y_{LQ} are related by the GUT boundary condition, Eq. (28). Moreover, as discussed in Appendix C, the RGE running does not affect their flavour structure, only the overall normalisation. Therefore, we see from Eq. (39) that the ratio between the rates of $\mu \to eee$ and $\mu \to e$ conversion in nuclei only depends on M_{LQ}/M_{Δ} :

$$BR(\mu \to eee) \simeq 0.0021 \left(\frac{M_{LQ}}{M_{\Delta}}\right)^4 CR(\mu \text{ Au} \to e \text{ Au}) \simeq 0.0049 \left(\frac{M_{LQ}}{M_{\Delta}}\right)^4 CR(\mu \text{ Al} \to e \text{ Al}),$$
(40)

where we employed the TeV-scale relation Eq. (29). It is then clear that measurements (or constraints) of different LFV processes can provide non-trivial information on the mass spectrum of the theory, to be combined with the constraints from gauge coupling unification and proton decay discussed in the previous section. This is also depicted in Figure 5, where we plot the ratio BR($\mu \to eee$)/CR(μ Al $\to e$ Al) (red points) as a function of M_{Δ}/M_{LQ} , varying the mass parameters within the 1σ -favoured region of the Model 2 fit reported in Section 3.2.

The figure also displays $\mathrm{BR}(\mu \to eee)/\mathrm{BR}(K_L \to \mu e)$ (blue points). In the latter case, the correlation is much less pronounced since the two processes depend on different combinations of the coupling matrices (see Eq. (39)), which are in turn affected by the uncertainty stemming from the neutrino parameters in Eq. (31). To produce Figure 5, we employ the fits provided in Refs. [80, 81] for the mixing angles and neutrino mass differences, while the poorly-constrained Dirac phase and the unknown Majorana phases of the PMNS have been uniformly varied within $[0, 2\pi)$, and we scanned the value of the lowest neutrino mass (assuming normal hierarchy) in the range $0.001\,\mathrm{eV} \le m_1 \le 0.1\,\mathrm{eV}$. The logarithm of the absolute strength of the coupling was varied uniformly in the range $-4.5 \le \log_{10}(|Y_\Delta^{11}|) \le -2$.

The same choice of parameters has been employed to generate the plots of Figure 6, where the rates of $\mu \to eee$, $\mu \, \text{Al} \to e \, \text{Al}$ and $K_L \to \mu e$ are compared to the present bounds and future experimental sensitivities reported in Table 4. As we can see, a large portion of the parameter space is already excluded and substantially more is within the sensitivity of the upcoming experiments, in particular Mu3e [65] and Mu2e/COMET [67, 68]. Therefore, unless

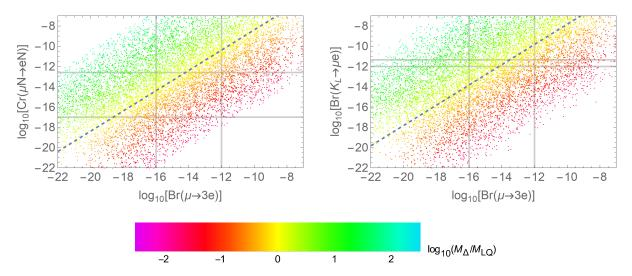


Figure 6: $CR(\mu Al \to e Al)$ vs $BR(\mu \to eee)$ (left panel) and $BR(K_L \to \mu e)$ vs $BR(\mu \to eee)$ (right panel) for the same variation of the parameters as in Figure 5 (see text for details). The colour of the points denotes the value of M_{Δ}/M_{LQ} , as indicated under the plots, and the dashed line corresponds to $M_{\Delta} = M_{LQ}$ and to setting the combinations of couplings appearing in Eq. (39) to their fitted central values. The gray lines indicate the present and future experimental limits as in Table 4. The present bound on $\mu \to e$ conversion was rescaled according to Eq. (40).

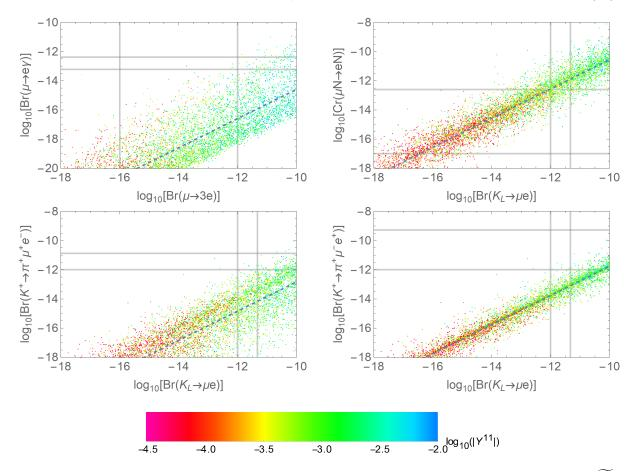


Figure 7: Correlations between processes induced by the exchange of the same field (Δ or R_2) for the same variation of the parameters as in Figures 5 and 6. The colour of the points denotes the value of $\log_{10}(|Y_{\Delta,LQ}^{11}|)$, as indicated under the plots. Lines as in Figure 6.

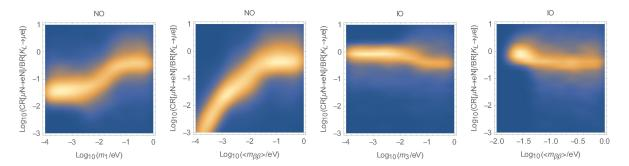


Figure 8: Ratio $CR(\mu Al \to e Al)/BR(K_L \to \mu e)$ as a function of the lowest neutrino mass and the effective Majorana neutrino mass obtained by marginalising over the other neutrino parameters. Left: normal ordering (NO). Right: inverted ordering (IO).

the overall size of the Yukawa couplings is considerably smaller than the range we considered, the spectrum of the model favoured by gauge coupling unification will likely provide positive LFV signals and, as Figures 5 and 6 show, such measurements would pinpoint the mass ratio M_{LQ}/M_{Δ} (besides measuring $|Y_{\Delta,LQ}^{21}|/Y_{\Delta,LQ}^{11}|/M_{\Delta,LQ}^{2}$, that is, the coefficients of the LFV operators induced by a triplet or a leptoquark exchange).

Of course, cleaner correlations are observed when considering pairs of processes induced by the same field, as shown in Figure 7. The first plot displays $\mu \to eee$ and $\mu \to e\gamma$, that is, processes due to the triplet Δ . The other three panels depict processes that are mediated by the leptoquark \widetilde{R}_2 . These plots also show how present and future experimental bounds can constrain the overall value of the Yukawa couplings.

The spread of the points in Figure 7 follows from the different combinations of the couplings relevant for different processes, as illustrated in Eq. (39), and thus is entirely due to the present uncertainty on the neutrino parameters in Eq. (31). This is a clear indication that measuring the rates of different LFV modes mediated by the same state from ϕ_{15} would provide precious information on the neutrino parameters beyond that that is currently available from the observation of neutrino oscillations and other neutrino experiments. However, the prospects of this programme do not seem very good in the case of the processes induced by Δ : the first panel of Figure 7 indeed shows that it is unlikely to observe $\mu \to e\gamma$ given the present constraint on $\mu \to eee$, which is a general feature of type II seesaw models irrespective of their possible GUT embedding.¹² Similarly, charged kaon decays (as shown in the second row of the figure) are not as promising as $K_L \to e\mu$. This latter mode, in combination with $\mu \to e$ in nuclei (see the second plot of Figure 7), seems instead to offer a suitable option to probe the flavour structure of Y_{LQ} , and thus of m_{ν} — especially if future experiments will be able to probe it substantially below the 10^{-12} level. Needless to say, a direct connection of these leptoquark-induced processes to the neutrino sector is possible only in presence of an underlying GUT structure as the one we are considering here (and it would be a crucial indication thereof).

We start studying the dependence of the ratio $CR(\mu Al \to e Al)/BR(K_L \to \mu e)$ on the parameters of the neutrino mass matrix m_{ν} . In Appendix D, we show the standard parametrisation that we employ for the PMNS matrix appearing in Eq. (31) and the dependence of this ratio of LFV rates on the 9 parameters of the neutrino sector. In particular, Figure 11 shows that measuring or constraining $CR(\mu Al \to e Al)/BR(K_L \to \mu e)$ would not provide useful information on the oscillation parameters, that is, the PMNS mixing angles, the neutrino mass splittings, and

This conclusion can be relaxed in specific cases where m_{ν} (and thus Y_{Δ}) features texture zeroes (see e.g. [82] for an assessment of such a possibility), for instance as a consequence of a flavour symmetry. In this kind of scenarios, one may envisage the possibility that either $Y_{\Delta}^{21} = 0$ or $Y_{\Delta}^{11} = 0$ at some high-energy scale related to new flavour dynamics and that the vanishing entry is only radiatively generated by running the matrix down to M_{Δ} through the RGEs shown in Appendix C. From Eq. (39) we see that this would suppress $\mu \to eee$ and make $\mu \to e\gamma$ comparatively more constraining. In the following, we do not further entertain a situation of this kind.

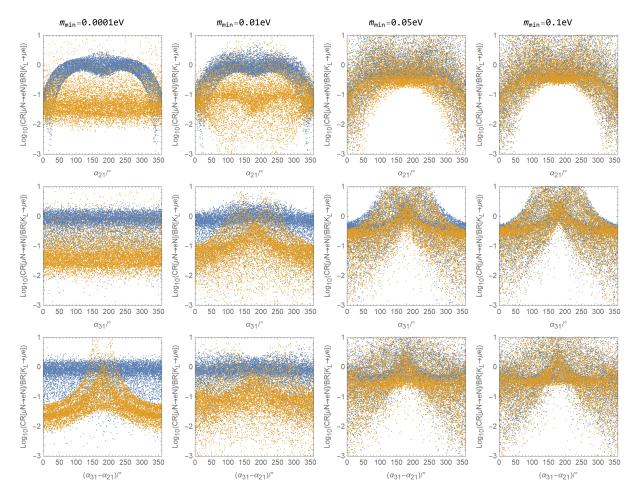


Figure 9: Ratio $CR(\mu Al \to e Al)/BR(K_L \to \mu e)$ as a function of the PMNS Majorana phases α_{21} (first row), α_{31} (second row), and the combination $(\alpha_{31} - \alpha_{21})$ (third row) obtained by marginalising over the other neutrino parameters [80] for different values of the lowest neutrino mass m_{\min} . The NO case is denoted by orange points, the IO case by blue points.

the Dirac CP-violating phase. In contrast, this ratio is very sensitive to parameters that are so far unknown: the two Majorana phases α_{21} and α_{31} , and the absolute neutrino mass m_{\min} , hence we focus here on these interesting quantities.

In Figure 8, we display the dependence of $CR(\mu Al \to e Al)/BR(K_L \to \mu e)$ on m_{\min} and the effective Majorana neutrino mass $\langle m_{\beta\beta} \rangle \equiv |\sum_i U_{ei}^2 m_i|$ —where U_{ei} are the first-row elements of the PMNS matrix in Eq. (56) — marginalised over the other neutrino parameters. This shows that, in the context of our GUT models, measuring $K_L \to \mu e$ with a rate more than 10 times larger than $\mu \to e$ conversion in nuclei would strongly disfavour the inverted ordering and, more importantly, point to a light absolute mass and effective mass, m_1 , $\langle m_{\beta\beta} \rangle \lesssim 10^{-2}$ eV, a situation rather challenging for other experimental probes such as searches for neutrinoless double-beta decays [83].

In Figure 9, we plot $CR(\mu Al \to e Al)/BR(K_L \to \mu e)$ as a function of the Majorana phases for different values of m_{\min} . These plots show how, within an underlying GUT structure, the comparison of these two LFV processes can shed light on the unknown Majorana phases, especially in presence of a future determination of (or a more stringent constraint on) m_{\min} . As an example, we can see that, for a relatively sizeable m_{\min} , $CR(\mu Al \to e Al) \ll BR(K_L \to \mu e)$ would require α_{21} to be quite close to 0. On the contrary, $CR(\mu Al \to e Al) \gg BR(K_L \to \mu e)$

¹³As customary, $m_{\min} = m_1$ for the normal mass ordering (NO), $m_1 < m_2 < m_3$, and $m_{\min} = m_3$, for the inverted mass ordering (IO), $m_3 < m_1 < m_2$.

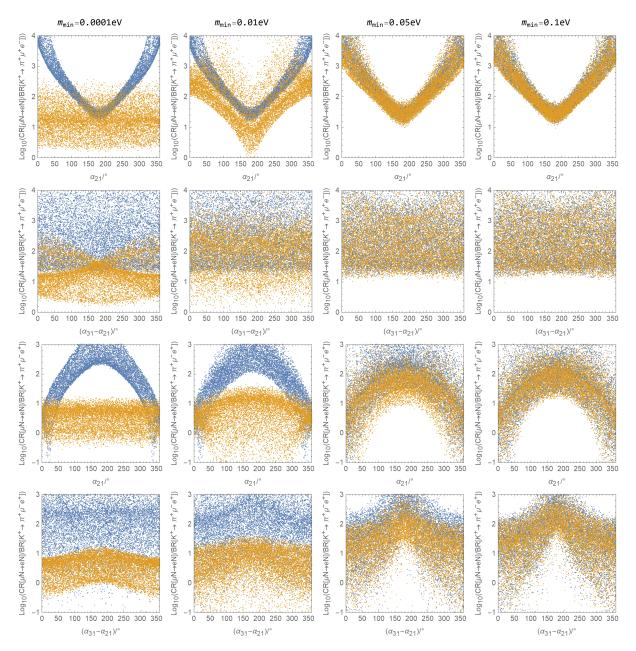


Figure 10: Same as Figure 9 for $CR(\mu Al \to e Al)/BR(K^+ \to \pi^+ \mu^+ e^-)$ (first and second row) and $CR(\mu Al \to e Al)/BR(K^+ \to \pi^+ \mu^- e^+)$ (third and fourth row).

would point to values of α_{31} not far from π . One can also see one of the phases becoming unphysical in the opposite limit $m_{\min} \to 0$.

Following from Eq. (39), the results of Figures 8 and 9 can be traced back to the change in the relative size of Y_{LQ}^{11} , Y_{LQ}^{12} , and Y_{LQ}^{22} for different values of m_{\min} , α_{21} and α_{31} . One can hence expect to obtain an even better sensitivity on these parameters by comparing $\mu \to e$ conversion in nuclei with charged kaon LFV modes, since the latter processes feature a simpler dependence on the couplings than K_L , without in particular interference terms, cf. Eq. (37). This is indeed shown by Figure 10 where similar results for $CR(\mu Al \to e Al)/BR(K^+ \to \pi^+\mu^+e^-)$ and $CR(\mu Al \to e Al)/BR(K^+ \to \pi^+\mu^-e^+)$ are displayed. As one can see, the complementarity of $K^+ \to \pi^+\mu^+e^-$ and $K^+ \to \pi^+\mu^-e^+$ in constraining α_{21} is particularly pronounced. However, fully exploiting the interplay of different kaon LFV modes would require a future search campaign able to reach sensitivities substantially below 10^{-12} , as shown by the second row of Figure 7.

5 Summary and conclusions

In this article, we have revisited a class of SU(5) GUT models with minimal field contents (see Table 1) that allow for successful unification of the gauge couplings and account for the origin of neutrino masses via type II seesaw. In Section 2, we classified our models based on how realistic fermion masses are achieved, studied their spectrum compatible with unification and p-decay constraints in Section 3, and finally discussed in detail their observable consequences in terms of LFV decays in Section 4.

The main findings of our study can be summarised as follows.

- The minimal SU(5) setup with non-renormalisable interactions ("Model 1") is excluded by proton decay searches, barring the case of fine cancellations triggered by a very peculiar flavour structure of the Yukawa couplings, hence it is strongly disfavoured, see Section 3.1.
- For what concerns models featuring vector-like matter ("Model 3"), we separately considered the case of a single $\mathbf{5} \oplus \overline{\mathbf{5}}$ fermionic representation and that with a single $\mathbf{10} \oplus \overline{\mathbf{10}}$. The former case is also strongly disfavoured by proton decay but it may become viable if multiple generations—at least 5—of vector-like fermions are introduced. The latter case is instead viable in its simplest form. However, the model is not predictive as the constraints on its spectrum are very loose and, in particular, no field is required to be light for the sake of unification and proton decay, cf. Section 3.3.
- The model with an additional scalar 45 and renormalisable interactions ("Model 2") can successfully achieve unification with a long enough proton lifetime and, especially in its minimal realisations, features very interesting predictions, as discussed at length in Section 3.2. Several fields are required to be light (that is, not much above the TeV scale), in particular the type II seesaw fields in the 15 representation that mediate LFV interactions.
- The couplings of these fields (the seesaw triplet Δ and its SU(5) partner, the scalar leptoquark \widetilde{R}_2) to SM fermions are linked to one another by the SU(5) structure and thus their LFV effects are related. From this it follows that measuring BR($\mu \to eee$)/CR($\mu N \to e N$) would pinpoint the mass ratio M_{Δ}/M_{LQ} , see Figure 5. Such a measurement (or constraint, in case only one of the two LFV processes is observed) could be then confronted with unification and p-decay constraints (as well as information from collider searches) in order to see if a consistent picture emerge.
- Instead, ratios of processes mediated by the same field (the most promising being $\mu \to e$ conversion in nuclei and $K_L \to \mu e$, both due to the leptoquark) provide information on the flavour structure of the couplings and thus directly on the neutrino mass matrix (in the charged-lepton mass basis), as both matrices Y_Δ and Y_{LQ} are proportional to m_ν . We showed that ratios of different LFV branching ratios can be particularly sensitive to the neutrino parameters that can not be measured through oscillation experiments, namely the Majorana phases and the absolute mass (see Figures 8-12).
- While some of our results apply to more general extensions of the SM featuring the triplet Δ (e.g. to a generic type II seesaw) or the leptoquark \widetilde{R}_2 , the connection between the processes induced by these two fields obviously requires the presence of a GUT. Our results show that measuring the rates of several LFV modes may allow to collect enough evidence of such a connection and thus of an underlying GUT structure.

Acknowledgments. LC is partially supported by the National Natural Science Foundation of China under the Grant No. 12035008.

A Scalar potential and scalar mass spectrum

We discuss here the feasibility of the scalar mass spectra characterised by large mass splittings among the states belonging to the same SU(5) representation that, according to the fit in Section 3, facilitate gauge coupling unification, and also if it is possible to achieve vev hierarchies in agreement with phenomenological requirements. In general, while the superpotential within supersymmetric SU(5) GUTs is strongly constrained by holomorphicity and renormalisability, that is not the case for a non-supersymmetric theory. In our scenarios, there are far more free parameters in the scalar potential, providing no fixed relationships among the masses of the new scalars and thus allowing (at the price of fine tunings) the large mass splittings assumed in Section 3.

A.1 ϕ_{24}

In our models, the dominant terms of the scalar potential dictating the ϕ_{24} components masses and the vacuum expectation value v_{24} read:

$$V_{24} = -\frac{1}{2}m_{24}^2 \text{Tr}[\phi_{24}^2] + \sqrt{\frac{10}{3}}\mu_{24} \text{Tr}[\phi_{24}^3] + \frac{1}{8}\lambda_1 \text{Tr}[\phi_{24}^2] \text{Tr}[\phi_{24}^2] + \frac{15}{2}\lambda_2 \text{Tr}[\phi_{24}^4]. \tag{41}$$

The interaction terms with ϕ_5 , ϕ_{15} , and ϕ_{45} are neglected here, as v_5 , $v_{15} \equiv v_{\Delta}$, $v_{45} \ll m_{24}$, v_{24} and the corresponding couplings are strongly suppressed after spontaneous symmetry breaking. Eq. (41) is in fact the same as the scalar potential in minimal SU(5) [84, 85]. Hence, requiring $\mu_{24} \rightarrow -4\lambda_2 v_{24}$, one can get:¹⁴

$$m_{\varrho_{1}}^{2} = (\lambda_{1} + 25\lambda_{2})v_{24}^{2}, \quad m_{\varrho_{8}}^{2} = 25\lambda_{2}v_{24}^{2}, \quad m_{\varrho_{3}}^{2} \to 0,$$

$$v_{\text{GUT}}^{2} \equiv v_{24}^{2} = \frac{2}{\lambda_{1} + 6\lambda_{2}}m_{24}^{2}.$$
(42)

These expression imply that the hierarchy $m_{\varrho_3} \ll m_{\varrho_8} \ll v_{24}$ is achievable, as required by the results of our fit. Furthermore, one can check that, in this case, $\frac{\partial^2 V_{24}}{\partial \phi_{24}^2} = \frac{2\lambda_1 + 20\lambda_2}{\lambda_1 + 6\lambda_2} m_{24}^2$ can be positive, so that v_{24} is really a local minimum.

A.2 ϕ_5 and ϕ_{45}

Both ϕ_5 and ϕ_{45} contain a SM-like Higgs doublet (respectively, H and H_2) and, due to $45 \otimes \bar{5} \supset 24$ the H- H_2 mixing term also exists. At low energies, this is a generic 2HDM where the masses of the heavy states are all free parameters, see e.g. [86]. For instance, the mass terms for the two neutral CP-even states are given by:

$$V(h_1, h_2) = \frac{1}{2} (m_{11}^2 h_1^2 + m_{22}^2 h_2^2 - 2m_{12}^2 h_1 h_2) + \text{quadratic terms},$$
 (43)

where m_{ij} are in general all at the GUT scale, if one does not invoke fine tuning. Then, the two local minima lie on:

$$v_5^2 \sim \mathcal{O}(\lambda^{-1}) \times (m_{11}^2 - m_{12}^2 \tan \beta),$$

 $v_{45}^2 \sim \mathcal{O}(\lambda^{-1}) \times (m_{22}^2 - m_{12}^2 \cot \beta),$ (44)

where $\tan \beta = v_{45}/v_5$ and all the quadratic coupling strengths are assumed to be at $\mathcal{O}(\lambda)$ for simplicity. As $v_{45}^2 + v_5^2 = v_{\rm EW}^2$ and $v_{45} \sim v_5$, one gets the following mass matrix for h_1, h_2 :

$$M_{h_1 h_2} = \begin{pmatrix} \tan \beta & -1 \\ -1 & \cot \beta \end{pmatrix} m_{12}^2 + \begin{pmatrix} \lambda_{11} & \lambda_{12} \\ \lambda_{21} & \lambda_{22} \end{pmatrix} v_{\text{EW}}^2.$$
 (45)

¹⁴For the components of ϕ_{24} , we adopt here the same conventions as in Ref. [85].

The contribution from the quadratic terms (due to EW-symmetry breaking) is taken into account in $\lambda_{ij}v_{\rm EW}^2$, where λ_{ij} are in general all $\mathcal{O}(\lambda)$. $M_{h_1h_2}$ has two eigenvalues: $m_{12}^2/(\cos\beta\sin\beta) \sim v_{\rm GUT}^2$ and $\mathcal{O}(\lambda)v_{\rm EW}^2$, corresponding to the squared mass of h_2 and h_1 individually. Therefore, due to the mixing, one can get the desired hierarchy between m_{h_2} and its vev v_{45} .

Strictly speaking, φ_3^S in ϕ_{45} could mix with the scalar triplet in ϕ_5 , but the mixing angle is independent of β so that both mass eigenstates can still be at GUT scale. This is because v_{24} is large and the cubic and quadratic interaction terms with ϕ_{24} should not be neglected here, providing more free parameters.¹⁵ Due to the same reason, the masses of the components of ϕ_5 and ϕ_{45} are all independent, which means that a light φ_8 , as required by the fit, is realisable without extending the model. For the explicit expressions, we refer to Section 4.1 of Ref. [85].

A.3 ϕ_{15}

The dominant scalar potential terms for the masses of the components of ϕ_{15} are:

$$V_{15} = -\frac{1}{2}m_{15}^2 \text{Tr}[\phi_{15}\phi_{15}^*] + \mu_{15} \text{Tr}[\phi_{15}\phi_{15}^*\phi_{24}] + b_1 \text{Tr}[\phi_{15}\phi_{15}^*] \text{Tr}[\phi_{24}\phi_{24}] + 30b_2 \text{Tr}[\phi_{15}\phi_{15}^*\phi_{24}\phi_{24}] + 15b_3 \text{Tr}[\phi_{15}\phi_{24}\phi_{15}^*\phi_{24}],$$

$$(46)$$

Again, when m_{Δ} , $m_{\widetilde{R_2}} \gg v_{\rm EW}$, the interactions with ϕ_5 , ϕ_{45} or the ϕ_{15} quadratic couplings can be neglected. After SU(5) breaking, the mass spectrum reads: ¹⁶

$$m_{\Delta}^{2} = -m_{15}^{2} + 6\mu_{15}v_{24} + 2b_{1}v_{24}^{2} + 18b_{2}v_{24}^{2} + 9b_{3}v_{24}^{2},$$

$$m_{\widetilde{R}_{2}}^{2} = -m_{15}^{2} + \mu_{15}v_{24} + 2b_{1}v_{24}^{2} + 13b_{2}v_{24}^{2} - 6b_{3}v_{24}^{2},$$

$$m_{S}^{2} = -m_{15}^{2} - 4\mu_{15}v_{24} + 2b_{1}v_{24}^{2} + 8b_{2}v_{24}^{2} + 4b_{3}v_{24}^{2}.$$

$$(47)$$

Resorting to fine tuning, $0 < m_{\Delta}^2 \sim m_{\widetilde{R}_2}^2 \ll m_S^2 \sim v_{24}^2$ is possible, as assumed in the rest of the paper. Furthermore, the cubic term in Eq. (30) gives a non-zero vacuum expectation value: $v_{\Delta} \sim \mu v_5^2/(\sqrt{2}m_{\Delta}^2)$, which is small (suppressed by m_{Δ}) as desired.

B More details on proton decay

B.1 Renormalisation of the baryon-number-violating operators

The renormalisation factor appearing in Eqs. (21-25) is given by $A = A_{LD}A_{SD}$, where A_{LD} and A_{SD} account for the long-distance and short-distance running of the baryon-number-violating operators, respectively, see e.g. [43]. The former one corresponds to the QCD running from m_t to the proton mass scale:

$$A_{LD} = \left(\frac{\alpha_3(m_p)}{\alpha_3(m_c)}\right)^{2/9} \left(\frac{\alpha_3(m_c)}{\alpha_3(m_b)}\right)^{6/25} \left(\frac{\alpha_3(m_b)}{\alpha_3(m_t)}\right)^{6/23} \approx 1.5.$$
 (48)

The short-distance contribution encodes the renormalisation of the operators from the GUT scale down to m_t . This can be given in terms of the running of the gauge couplings, that is, in terms of the SM β -function coefficients plus the contribution of the extra fields:

$$A_{SD} = \left(\frac{\alpha_{1}(m_{t})}{\alpha_{1}(M_{I})}\right)^{-\frac{23}{30b_{1}^{\text{SM}}}} \left(\frac{\alpha_{2}(m_{t})}{\alpha_{2}(M_{I})}\right)^{-\frac{3}{2b_{2}^{\text{SM}}}} \left(\frac{\alpha_{3}(m_{t})}{\alpha_{3}(M_{I})}\right)^{-\frac{4}{3b_{3}^{\text{SM}}}} \times \left(\frac{\alpha_{1}(M_{I})}{\alpha_{\text{GUT}}}\right)^{-\frac{23}{30(b_{1}^{\text{SM}}+\Delta b_{1})}} \left(\frac{\alpha_{2}(M_{I})}{\alpha_{\text{GUT}}}\right)^{-\frac{3}{2(b_{2}^{\text{SM}}+\Delta b_{2})}} \left(\frac{\alpha_{3}(M_{I})}{\alpha_{\text{GUT}}}\right)^{-\frac{4}{3(b_{3}^{\text{SM}}+\Delta b_{3})}},$$
(49)

$$^{16}\phi_{15} = \begin{pmatrix} S & \widetilde{R_2}/\sqrt{2} \\ \widetilde{R_2}/\sqrt{2} & i\sigma_2\Delta \end{pmatrix}$$
, with Δ and $\widetilde{R_2}$ shown in Eq. (27).

¹⁵The coupling to ϕ_{15} is not dominant as custodial symmetry requires $v_{15} \ll v_{EW}$.

where we considered the extra matter at a single intermediate scale M_I (with $\Delta b_i \equiv \sum_I b_i^I$), the generalization to multiple thresholds being straightforward. To obtain an estimate of the typical value of A_{SD} , one can consider only the contributions from b_i^{SM} in the above equation and take $\alpha_{\text{GUT}} = 1/25$, which gives $A_{SD} \approx 1.3$.

B.2 Proton decay matrix elements

A recent lattice QCD evaluation of the hadronic matrix elements in Eqs. (21-25) gives [87]:

$$\langle \pi^{0} | (ud)_{R} u_{L} | p \rangle = -0.131(4)(13) \,\text{GeV}^{2} \,, \qquad \langle \pi^{0} | (ud)_{L} u_{L} | p \rangle = 0.134(5)(16) \,\text{GeV}^{2} \,,
\langle K^{0} | (us)_{R} u_{L} | p \rangle = 0.103(3)(11) \,\text{GeV}^{2} \,, \qquad \langle K^{0} | (us)_{L} u_{L} | p \rangle = 0.057(2)(6) \,\text{GeV}^{2} \,,
\langle \pi^{+} | (du)_{R} d_{L} | p \rangle = -0.186(6)(18) \,\text{GeV}^{2} \,,
\langle K^{+} | (us)_{R} d_{L} | p \rangle = -0.049(2)(5) \,\text{GeV}^{2} \,, \qquad \langle K^{+} | (ud)_{R} s_{L} | p \rangle = -0.134(4)(14) \,\text{GeV}^{2} \,.$$
(50)

B.3 Other possible contributions to proton decay

As neutrinos are Majorana particles following the type II seesaw mechanism, the proton could also decay to a meson and a lepton (instead of an antilepton), thus breaking B - L. However, these processes are strongly suppressed by the small neutrino mass, as we will show below.

According to Eq. (26), the leptoquark R_2 can convert a down-type quark to a lepton and induce B-L violating proton decay processes (such as $p \to \pi^+\nu$) by interacting with other scalar fields via $\mu\phi_5^i\phi_5^j(\phi_{15}^*)_{ij}$. The resulting d=7 effective operator, which has been already discussed in Ref. [10], reads:

$$\mathcal{O}_{d=7} = \frac{\mu Y_{d\ell} Y_{LQ}^{\dagger}}{M_T^2 M_{LQ}^2} \overline{U_R^c} D_R \overline{L_L} D_R H^*. \tag{51}$$

where M_T is the mass of the colour triplet $(\bar{\bf 3}, {\bf 1}, -1/3)$ in $\phi_{\bf 5}$ that also generates the standard B-L conserving contributions to proton decay via the d=6 operator:

$$\mathcal{O}_{d=6} = \frac{Y_{d\ell}Y_{d\ell}^{\dagger}}{M_T^c} \overline{U_R^c} D_R \overline{L_L^c} Q_L. \tag{52}$$

Hence, in order to make sure that the processes induced by $\mathcal{O}_{d=7}$ are as suppressed as the ones from $\mathcal{O}_{d=6}$, we need to require that $\mu \, v_{\rm EW} Y_{LQ}/M_{LQ}^2 \lesssim Y_{d\ell}$. Relating these parameters to the effective Majorana neutrino mass $\langle m_{\beta\beta} \rangle \sim Y_{\Delta} v_{\Delta} \sim Y_{\Delta} \frac{\mu \, v_{\rm EW}^2}{M_{\Delta}^2} \sim Y_{LQ} \frac{\mu \, v_{\rm EW}^2}{M_{\Delta}^2}$ and to the charged lepton masses $m_{\ell} \sim v_{\rm EW} Y_{d\ell}$, the condition becomes:

$$\langle m_{\beta\beta} \rangle \times \frac{M_{\Delta}^2}{M_{LO}^2} \lesssim m_{\ell} \,.$$
 (53)

According to the Bayesian analysis in Section 3.2, TeV-scale masses for both Δ and R_2 are favoured, then Eq. (53) is always verified. In other words, the smallness of the absolute neutrino mass further suppresses the B-L violating processes relative to the ordinary proton decay induced by the colour triplet. Notice that, taking $\langle m_{\beta\beta} \rangle = 0.1$ eV and $m_{\ell} = m_e$, the above condition is still fulfilled up to $M_{\Delta} \approx 2000 \times M_{LQ}$. For values of M_{Δ} larger than that, the induced proton decay could still evade the experimental bounds, considering that the processes mediated by the colour triplet with $M_T = M_{\text{GUT}}$ are suppressed compared to those induced by the SU(5) gauge bosons, since the Yukawa couplings in $Y_{d\ell}$ and Y_{LQ} are much smaller than the unified gauge coupling strength—the latter couplings being severely constrained by LFV processes, as discussed in Section 4.

C RGEs of triplet and leptoquark Yukawa couplings

The 1-loop RGEs for the Eq. (26) interactions related to type II seesaw are given by [88, 89]:

$$(4\pi)^{2} \frac{dY_{\Delta}}{dt} = \left[-\frac{9}{10} g_{1}^{2} - \frac{9}{2} g_{2}^{2} + \text{Tr} \left(Y_{\Delta}^{\dagger} Y_{\Delta} \right) \right] Y_{\Delta} + \left[3 Y_{\Delta} Y_{\Delta}^{\dagger} Y_{\Delta} + \frac{1}{2} Y_{\ell}^{T} Y_{\ell}^{*} Y_{\Delta} + \frac{1}{2} Y_{\Delta} Y_{\ell}^{\dagger} Y_{\ell} \right] ,$$

$$(4\pi)^{2} \frac{dY_{LQ}}{dt} = \left[-\frac{13}{20} g_{1}^{2} - \frac{9}{4} g_{2}^{2} - 4g_{3}^{2} + \text{Tr} \left(Y_{LQ}^{\dagger} Y_{LQ} \right) \right] Y_{LQ} + \left[\frac{5}{2} Y_{LQ} Y_{LQ}^{\dagger} Y_{LQ} + Y_{d} Y_{d}^{\dagger} Y_{LQ} + \frac{1}{2} Y_{LQ} Y_{\ell}^{\dagger} Y_{\ell} \right] ,$$

$$(55)$$

where $t \equiv \ln(\mu/m_Z)$. As one can see, Y_{LQ} runs more than Y_{Δ} due to the term $\propto g_3^2$, reflecting the fact that the leptoquark is strongly interacting while the triplet Δ is colour neutral. As a consequence the GUT relation $Y_{LQ} = \sqrt{2} \, Y_{\Delta}$ does not hold at lower energies. On the other hand, notice that the flavour structure of the matrices can be only changed by the cubic terms $\propto Y_{\Delta} Y_{\Delta}^{\dagger} Y_{\Delta}$ and $Y_{LQ} Y_{LQ}^{\dagger} Y_{LQ}$. For the light spectra we are interested in, LFV processes constrain the entries of Y_{Δ} and Y_{LQ} to be rather small, as discussed in Section 4.2, hence the effect of these terms is negligible and the flavour structure of the two matrices will remain the same at all scales to a very good approximation.

Solving the above RGEs for a typical Model 2 spectrum, $M_{\varrho_3}=M_{\Delta}=M_{LQ}=M_{\varphi_8}=1$ TeV (implying $M_{\varrho_8}\approx 1.3\times 10^{15}$ GeV, $M_{\text{GUT}}\approx 2.5\times 10^{15}$ GeV, $\alpha_{\text{GUT}}^{-1}\approx 33$), one obtains $Y_{LQ}(M_{LQ})/Y_{LQ}(M_{\text{GUT}})\approx 2.4$ and $Y_{\Delta}(M_{\Delta})/Y_{\Delta}(M_{\text{GUT}})\approx 1.6$, which results in the low-energy relation $Y_{LQ}\approx 2.1\,Y_{\Delta}$. Since this result is not much affected by details of the spectrum, we employed this constant factor in the numerical analysis of Section 4.

D Dependence of the LFV rates on neutrino parameters

The PMNS matrix in Eq. (32) reads:

$$U_{\text{PMNS}} = \begin{pmatrix} 1 & 0 & 0 \\ 0 & c_{23} & s_{23} \\ 0 & -s_{23} & c_{23} \end{pmatrix} \begin{pmatrix} c_{13} & 0 & e^{-i\delta_D} s_{13} \\ 0 & 1 & 0 \\ -e^{i\delta_D} s_{13} & 0 & c_{13} \end{pmatrix} \begin{pmatrix} c_{12} & s_{12} & 0 \\ -s_{12} & c_{12} & 0 \\ 0 & 0 & 1 \end{pmatrix} \cdot P, \quad (56)$$

where $s_{ij} \equiv \sin \theta_{ij}$, $c_{ij} \equiv \cos \theta_{ij}$ and P is the matrix containing the Majorana phases:

$$P \equiv \operatorname{diag}(1, e^{-i\alpha_{21}/2}, e^{-i\alpha_{31}/2}). \tag{57}$$

Besides the six parameters in the PMNS, the neutrino sector comprises three mass parameters, namely the mass splittings Δ_{21} and Δ_{31} (with $\Delta_{ij} \equiv m_i^2 - m_j^2$) and the absolute mass $m_{\min} = m_1$ [NO], m_3 [IO].

In Figure 11, we show the dependence of the ratio $CR(\mu Al \to e Al)/BR(K_L \to \mu e)$ on the above-defined parameters for the normal ordering case and the oscillation parameters resulting from the fit in Refs. [80, 81]. Pronounced effects are observed only in the case of the Majorana phases and the absolute neutrino mass.

For completeness, we show in Figure 12 the same analysis for $BR(\mu \to e\gamma)/BR(\mu \to eee)$, which exhibits a strong sensitivity on m_1 but not a very prominent one on the phases. It is interesting to notice that Figure 12 displays general results for type II seesaw, independent of our specific GUT models. This shows that, in case of a positive signal for $\mu \to eee$ at Mu3e [65], a future experiment able to go substantially beyond the sensitivity of MEGII [63] on $\mu \to e\gamma$ (for ideas in this sense see Ref. [90]) would be particularly sensitive to a very light absolute mass.

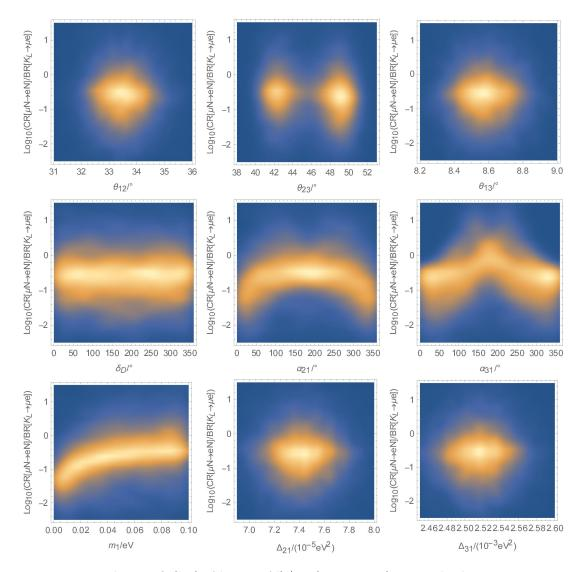


Figure 11: Dependence of $CR(\mu Al \to e Al)/BR(K_L \to \mu e)$ on each the 9 neutrino sector parameters defined in Appendix D marginalised over the other parameters for the NO case. The results of the fit for the three oscillation angles and the two mass splittings reported in [80, 81] have been employed here.

References

- [1] H. Georgi and S. L. Glashow, Unity of All Elementary Particle Forces, Phys. Rev. Lett. 32 (1974) 438–441.
- [2] H. Fritzsch and P. Minkowski, *Unified Interactions of Leptons and Hadrons, Annals Phys.* **93** (1975) 193–266.
- [3] D. Croon, T. E. Gonzalo, L. Graf, N. Košnik and G. White, GUT Physics in the era of the LHC, Front. in Phys. 7 (2019) 76, [1903.04977].
- [4] A. Abada, C. Biggio, F. Bonnet, M. B. Gavela and T. Hambye, Low energy effects of neutrino masses, JHEP 12 (2007) 061, [0707.4058].
- [5] Y. Cai, J. Herrero-García, M. A. Schmidt, A. Vicente and R. R. Volkas, From the trees to the forest: a review of radiative neutrino mass models, Front. in Phys. 5 (2017) 63, [1706.08524].

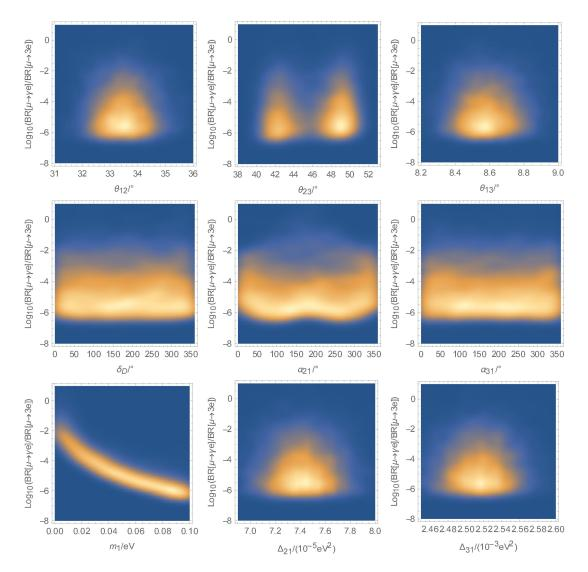


Figure 12: Same as Figure 11 for $BR(\mu \to e\gamma)/BR(\mu \to eee)$.

- [6] M. Magg and C. Wetterich, Neutrino Mass Problem and Gauge Hierarchy, Phys. Lett. B 94 (1980) 61–64.
- [7] G. Lazarides, Q. Shafi and C. Wetterich, Proton Lifetime and Fermion Masses in an SO(10) Model, Nucl. Phys. B 181 (1981) 287–300.
- [8] R. N. Mohapatra and G. Senjanovic, Neutrino Masses and Mixings in Gauge Models with Spontaneous Parity Violation, Phys. Rev. D 23 (1981) 165.
- [9] J. Schechter and J. W. F. Valle, Neutrino Masses in SU(2) x U(1) Theories, Phys. Rev. D 22 (1980) 2227.
- [10] I. Dorsner and P. Fileviez Perez, Unification without supersymmetry: Neutrino mass, proton decay and light leptoquarks, Nucl. Phys. B 723 (2005) 53–76, [hep-ph/0504276].
- [11] I. Dorsner, P. Fileviez Perez and R. Gonzalez Felipe, Phenomenological and cosmological aspects of a minimal GUT scenario, Nucl. Phys. B 747 (2006) 312–327, [hep-ph/0512068].
- [12] I. Dorsner and P. Fileviez Perez, Unification versus proton decay in SU(5), Phys. Lett. B 642 (2006) 248–252, [hep-ph/0606062].

- [13] I. Dorsner, P. Fileviez Perez and G. Rodrigo, Fermion masses and the UV cutoff of the minimal realistic SU(5), Phys. Rev. D 75 (2007) 125007, [hep-ph/0607208].
- [14] I. Dorsner and I. Mocioiu, *Predictions from type II see-saw mechanism in SU(5)*, *Nucl. Phys. B* **796** (2008) 123–136, [0708.3332].
- [15] P. Fileviez Perez, T. Han, T. Li and M. J. Ramsey-Musolf, Leptoquarks and Neutrino Masses at the LHC, Nucl. Phys. B 819 (2009) 139–176, [0810.4138].
- [16] S. Antusch, K. Hinze and S. Saad, Viable quark-lepton Yukawa ratios and nucleon decay predictions in SU(5) GUTs with type-II seesaw, 2205.01120.
- [17] B. Bajc and G. Senjanovic, Seesaw at LHC, JHEP 08 (2007) 014, [hep-ph/0612029].
- [18] I. Dorsner and P. Fileviez Perez, Upper Bound on the Mass of the Type III Seesaw Triplet in an SU(5) Model, JHEP 06 (2007) 029, [hep-ph/0612216].
- [19] B. Bajc, M. Nemevsek and G. Senjanovic, Probing seesaw at LHC, Phys. Rev. D 76 (2007) 055011, [hep-ph/0703080].
- [20] P. Fileviez Perez, Renormalizable adjoint SU(5), Phys. Lett. B 654 (2007) 189–193, [hep-ph/0702287].
- [21] A. Arhrib, B. Bajc, D. K. Ghosh, T. Han, G.-Y. Huang, I. Puljak et al., Collider Signatures for Heavy Lepton Triplet in Type I+III Seesaw, Phys. Rev. D 82 (2010) 053004, [0904.2390].
- [22] P. Fileviez Pérez, A. Gross and C. Murgui, Seesaw scale, unification, and proton decay, Phys. Rev. D 98 (2018) 035032, [1804.07831].
- [23] U. C. Olivas, K. Kowalska and D. Kumar, Road map through the desert with scalars, 2112.11742.
- [24] L. Calibbi and G. Signorelli, Charged Lepton Flavour Violation: An Experimental and Theoretical Introduction, Riv. Nuovo Cim. 41 (2018) 71–174, [1709.00294].
- [25] N. D. Barrie, C. Han and H. Murayama, Affleck-Dine Leptogenesis from Higgs Inflation, Phys. Rev. Lett. 128 (2022) 141801, [2106.03381].
- [26] N. D. Barrie, C. Han and H. Murayama, Type II Seesaw leptogenesis, JHEP 05 (2022) 160, [2204.08202].
- [27] I. Doršner, S. Fajfer, A. Greljo, J. F. Kamenik and N. Košnik, *Physics of leptoquarks in precision experiments and at particle colliders*, *Phys. Rept.* **641** (2016) 1–68, [1603.04993].
- [28] G.-y. Huang and S. Zhou, Precise Values of Running Quark and Lepton Masses in the Standard Model, Phys. Rev. D 103 (2021) 016010, [2009.04851].
- [29] S. Antusch and V. Maurer, Running quark and lepton parameters at various scales, JHEP 11 (2013) 115, [1306.6879].
- [30] J. R. Ellis and M. K. Gaillard, Fermion Masses and Higgs Representations in SU(5), Phys. Lett. B 88 (1979) 315–319.
- [31] E. Witten, Neutrino Masses in the Minimal O(10) Theory, Phys. Lett. B 91 (1980) 81–84.
- [32] I. Dorsner, S. Fajfer and I. Mustac, Light vector-like fermions in a minimal SU(5) setup, Phys. Rev. D 89 (2014) 115004, [1401.6870].

- [33] K. S. Babu, B. Bajc and Z. Tavartkiladze, Realistic Fermion Masses and Nucleon Decay Rates in SUSY SU(5) with Vector-Like Matter, Phys. Rev. D 86 (2012) 075005, [1207.6388].
- [34] A. Giveon, L. J. Hall and U. Sarid, SU(5) unification revisited, Phys. Lett. B **271** (1991) 138–144.
- [35] M. E. Machacek and M. T. Vaughn, Two Loop Renormalization Group Equations in a General Quantum Field Theory. 1. Wave Function Renormalization, Nucl. Phys. B 222 (1983) 83–103.
- [36] Particle Data Group collaboration, P. Zyla et al., Review of Particle Physics, PTEP **2020** (2020) 083C01.
- [37] M. L. Alciati, F. Feruglio, Y. Lin and A. Varagnolo, *Proton lifetime from SU(5)* unification in extra dimensions, *JHEP* **03** (2005) 054, [hep-ph/0501086].
- [38] SUPER-KAMIOKANDE collaboration, A. Takenaka et al., Search for proton decay via $p \to e^+\pi^0$ and $p \to \mu^+\pi^0$ with an enlarged fiducial volume in Super-Kamiokande I-IV, Phys. Rev. D 102 (2020) 112011, [2010.16098].
- [39] SUPER-KAMIOKANDE collaboration, K. Kobayashi et al., Search for nucleon decay via modes favored by supersymmetric grand unification models in Super-Kamiokande-I, Phys. Rev. D 72 (2005) 052007, [hep-ex/0502026].
- [40] SUPER-KAMIOKANDE collaboration, R. Matsumoto et al., Search for proton decay via $p \to \mu^+ K^0$ in 0.37 megaton-years exposure of Super-Kamiokande, 2208.13188.
- [41] SUPER-KAMIOKANDE collaboration, K. Abe et al., Search for Nucleon Decay via $n \to \bar{\nu}\pi^0$ and $p \to \bar{\nu}\pi^+$ in Super-Kamiokande, Phys. Rev. Lett. 113 (2014) 121802, [1305.4391].
- [42] SUPER-KAMIOKANDE collaboration, K. Abe et al., Search for proton decay via $p \to \nu K^+$ using 260 kiloton-year data of Super-Kamiokande, Phys. Rev. D **90** (2014) 072005, [1408.1195].
- [43] P. Nath and P. Fileviez Perez, Proton stability in grand unified theories, in strings and in branes, Phys. Rept. 441 (2007) 191–317, [hep-ph/0601023].
- [44] I. Dorsner and P. Fileviez Perez, How long could we live?, Phys. Lett. B 625 (2005) 88–95, [hep-ph/0410198].
- [45] CDF collaboration, T. Aaltonen et al., High-precision measurement of the W boson mass with the CDF II detector, Science 376 (2022) 170–176.
- [46] L. Di Luzio, R. Gröber and P. Paradisi, Higgs physics confronts the M_W anomaly, 2204.05284.
- [47] J. L. Evans, T. T. Yanagida and N. Yokozaki, W boson mass anomaly and grand unification, 2205.03877.
- [48] G. Senjanović and M. Zantedeschi, SU(5) grand unification and W-boson mass, 2205.05022.
- [49] JUNO collaboration, Z. Djurcic et al., JUNO Conceptual Design Report, 1508.07166.
- [50] DUNE collaboration, R. Acciarri et al., Long-Baseline Neutrino Facility (LBNF) and Deep Underground Neutrino Experiment (DUNE): Conceptual Design Report, Volume 2: The Physics Program for DUNE at LBNF, 1512.06148.

- [51] HYPER-KAMIOKANDE collaboration, K. Abe et al., *Hyper-Kamiokande Design Report*, 1805.04163.
- [52] S. Ashanujjaman and K. Ghosh, Revisiting type-II see-saw: present limits and future prospects at LHC, JHEP 03 (2022) 195, [2108.10952].
- [53] ATLAS collaboration, M. Aaboud et al., Search for doubly charged Higgs boson production in multi-lepton final states with the ATLAS detector using proton-proton collisions at $\sqrt{s} = 13$ TeV, Eur. Phys. J. C 78 (2018) 199, [1710.09748].
- [54] ATLAS collaboration, G. Aad et al., Search for doubly and singly charged Higgs bosons decaying into vector bosons in multi-lepton final states with the ATLAS detector using proton-proton collisions at $\sqrt{s} = 13$ TeV, JHEP **06** (2021) 146, [2101.11961].
- [55] ATLAS collaboration, G. Aad et al., Search for pairs of scalar leptoquarks decaying into quarks and electrons or muons in $\sqrt{s} = 13$ TeV pp collisions with the ATLAS detector, JHEP 10 (2020) 112, [2006.05872].
- [56] A. V. Manohar and M. B. Wise, Flavor changing neutral currents, an extended scalar sector, and the Higgs production rate at the CERN LHC, Phys. Rev. D 74 (2006) 035009, [hep-ph/0606172].
- [57] L. Darmé, B. Fuks and M. Goodsell, Cornering sgluons with four-top-quark events, Phys. Lett. B 784 (2018) 223–228, [1805.10835].
- [58] V. Miralles and A. Pich, LHC bounds on colored scalars, Phys. Rev. D 100 (2019) 115042, [1910.07947].
- [59] G. Cacciapaglia, A. Deandrea, T. Flacke and A. M. Iyer, Gluon-Photon Signatures for color octet at the LHC (and beyond), JHEP 05 (2020) 027, [2002.01474].
- [60] CMS collaboration, A. M. Sirunyan et al., Search for narrow and broad dijet resonances in proton-proton collisions at $\sqrt{s} = 13$ TeV and constraints on dark matter mediators and other new particles, JHEP 08 (2018) 130, [1806.00843].
- [61] S. Kanemura and K. Yagyu, Implication of the W boson mass anomaly at CDF II in the Higgs triplet model with a mass difference, 2204.07511.
- [62] MEG collaboration, A. M. Baldini et al., Search for the lepton flavour violating decay $\mu^+ \to e^+ \gamma$ with the full dataset of the MEG experiment, Eur. Phys. J. C **76** (2016) 434, [1605.05081].
- [63] MEG II collaboration, A. Baldini et al., The design of the MEG II experiment, Eur. Phys. J. C 78 (2018) 380, [1801.04688].
- [64] SINDRUM collaboration, U. Bellgardt et al., Search for the Decay $\mu^+ \to e^+e^+e^-$, Nucl. Phys. B 299 (1988) 1–6.
- [65] A. Blondel et al., Research Proposal for an Experiment to Search for the Decay $\mu \to eee$, 1301.6113.
- [66] SINDRUM II collaboration, W. H. Bertl et al., A Search for muon to electron conversion in muonic gold, Eur. Phys. J. C 47 (2006) 337–346.
- [67] Mu2E collaboration, L. Bartoszek et al., Mu2e Technical Design Report, 1501.05241.
- [68] COMET collaboration, Y. Kuno, A search for muon-to-electron conversion at J-PARC: The COMET experiment, PTEP 2013 (2013) 022C01.

- [69] BNL collaboration, D. Ambrose et al., New limit on muon and electron lepton number violation from KO(L) —> mu+-e-+ decay, Phys. Rev. Lett. **81** (1998) 5734–5737, [hep-ex/9811038].
- [70] E. Goudzovski et al., New Physics Searches at Kaon and Hyperon Factories, 2201.07805.
- [71] KTEV collaboration, E. Abouzaid et al., Search for lepton flavor violating decays of the neutral kaon, Phys. Rev. Lett. 100 (2008) 131803, [0711.3472].
- [72] A. Sher et al., An Improved upper limit on the decay $K+ \longrightarrow pi+ mu+ e-$, Phys. Rev. D **72** (2005) 012005, [hep-ex/0502020].
- [73] R. Appel et al., Search for lepton flavor violation in K+ decays, Phys. Rev. Lett. 85 (2000) 2877–2880, [hep-ex/0006003].
- [74] R. Kitano, M. Koike and Y. Okada, Detailed calculation of lepton flavor violating muon electron conversion rate for various nuclei, Phys. Rev. D 66 (2002) 096002, [hep-ph/0203110].
- [75] J. Heeck, R. Szafron and Y. Uesaka, *Isotope dependence of muon-to-electron conversion*, 2203.00702.
- [76] D. Bečirević, O. Sumensari and R. Zukanovich Funchal, Lepton flavor violation in exclusive $b \rightarrow s$ decays, Eur. Phys. J. C **76** (2016) 134, [1602.00881].
- [77] V. Cirigliano, G. Ecker, H. Neufeld, A. Pich and J. Portoles, Kaon Decays in the Standard Model, Rev. Mod. Phys. 84 (2012) 399, [1107.6001].
- [78] KTEV collaboration, T. Alexopoulos et al., Measurements of semileptonic K(L) decay form-factors, Phys. Rev. D 70 (2004) 092007, [hep-ex/0406003].
- [79] FLAVOUR LATTICE AVERAGING GROUP collaboration, S. Aoki et al., FLAG Review 2019: Flavour Lattice Averaging Group (FLAG), Eur. Phys. J. C 80 (2020) 113, [1902.08191].
- [80] I. Esteban, M. C. Gonzalez-Garcia, M. Maltoni, T. Schwetz and A. Zhou, The fate of hints: updated global analysis of three-flavor neutrino oscillations, JHEP 09 (2020) 178, [2007.14792].
- [81] I. Esteban, M. C. Gonzalez-Garcia, M. Maltoni, T. Schwetz and A. Zhou, "NuFIT 5.1 (2021)." http://www.nu-fit.org.
- [82] S. Zhou, Update on two-zero textures of the Majorana neutrino mass matrix in light of recent T2K, Super-Kamiokande and NOνA results, Chin. Phys. C 40 (2016) 033102, [1509.05300].
- [83] M. Agostini, G. Benato, J. A. Detwiler, J. Menéndez and F. Vissani, *Toward the discovery of matter creation with neutrinoless double-beta decay*, 2202.01787.
- [84] A. H. Guth and E. J. Weinberg, Cosmological Consequences of a First Order Phase Transition in the SU(5) Grand Unified Model, Phys. Rev. D 23 (1981) 876.
- [85] K. Kumericki, T. Mede and I. Picek, Renormalizable SU(5) Completions of a Zee-type Neutrino Mass Model, Phys. Rev. D 97 (2018) 055012, [1712.05246].
- [86] G. C. Branco, P. M. Ferreira, L. Lavoura, M. N. Rebelo, M. Sher and J. P. Silva, Theory and phenomenology of two-Higgs-doublet models, Phys. Rept. 516 (2012) 1–102, [1106.0034].

- [87] Y. Aoki, T. Izubuchi, E. Shintani and A. Soni, Improved lattice computation of proton decay matrix elements, Phys. Rev. D 96 (2017) 014506, [1705.01338].
- [88] M. A. Schmidt, Renormalization group evolution in the type I+II seesaw model, Phys. Rev. D **76** (2007) 073010, [0705.3841].
- [89] P. Bandyopadhyay, S. Jangid and A. Karan, Constraining Scalar Doublet and Triplet Leptoquarks with Vacuum Stability and Perturbativity, 2111.03872.
- [90] M. Aoki et al., A New Charged Lepton Flavor Violation Program at Fermilab, in 2022 Snowmass Summer Study, 3, 2022, 2203.08278.